AD-A049 168 CATHOLIC UNIV OF AMERICA WASHINGTON D C VITREOUS STA--ETC F/G 20/6
DEVELOPMENT OF A LOW LOSS OPTICAL FIBER WITH A PARABOLIC PROFIL--ETC(U)
NOV 77 R K MOHR, P B MACEDO, T A LITOVITZ N00019-76-C-0674

UNCLASSIFIED NL

1 OF
AD
A049 168

END
DATE
FILMED
2-78
DDC

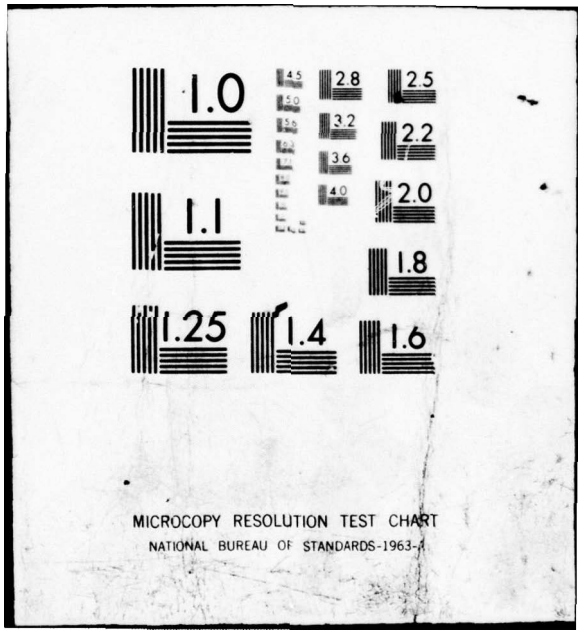
1.0
1.1
1.25
1.4
1.6
1.8
2.0
2.2
2.5
2.8
3.2
3.6
4.0
4.5
5.0
MICROCOPY RESOLUTION TEST CHART
NATIONAL BUREAU OF STANDARDS-1963-A

DEVELOPMENT OF A LOW LOSS OPTICAL FIBER WITH A PARABOLIC PROFILE

Unclassified

SECURITY CLASSIFICATION OF THIS PAGE (When Data Entered)

REPORT DOCUMENTATION PAGE

READ INSTRUCTIONS BEFORE COMPLETING FORM

1. REPORT NUMBER: FINAL REPORT	2. GOVT ACCESSION NO.
3. RECIPIENT'S CATALOG NUMBER	
4. TITLE (and Subtitle): DEVELOPMENT OF A LOW LOSS OPTICAL FIBER WITH A PARABOLIC PROFILE.	5. TYPE OF REPORT & PERIOD COVERED: Final Report. 1 Sep 76-30 Apr 77 9/1/76 - 4/30/77
	6. PERFORMING ORG. REPORT NUMBER
7. AUTHOR(s): R.K. Mohr, P.B. Macedo, [redacted] T.A. Litovitz	8. CONTRACT OR GRANT NUMBER(s): N00019-76-C-0674, N00019-76-C-0083
9. PERFORMING ORGANIZATION NAME AND ADDRESS: Catholic University of America, 620 Michigan Ave. NE, Washington, DC 20064	10. PROGRAM ELEMENT, PROJECT, TASK AREA & WORK UNIT NUMBERS
11. CONTROLLING OFFICE NAME AND ADDRESS: Vitreous State Laboratory, Catholic University, Washington, DC 20064	12. REPORT DATE: Nov [redacted] 77
	13. NUMBER OF PAGES
14. MONITORING AGENCY NAME & ADDRESS (if different from Controlling Office)	15. SECURITY CLASS. (of this report): Unclassified (12) 67p.
	15a. DECLASSIFICATION/DOWNGRADING SCHEDULE

16. DISTRIBUTION STATEMENT (of this Report)

~~Reproduction in whole or in part is permitted for any purpose of the United States Government.~~

APPROVED FOR PUBLIC RELEASE: DISTRIBUTION UNLIMITED

17. DISTRIBUTION STATEMENT (of the abstract entered in Block 20, if different from Report)

18. SUPPLEMENTARY NOTES

DDC RECEIVED JAN 27 1978 A

19. KEY WORDS (Continue on reverse side if necessary and identify by block number)

20. ABSTRACT (Continue on reverse side if necessary and identify by block number)

This is the final report of work completed under contract No. N00019-76-C-0674. The objective of this contract was to develop the technique of Molecular Stuffing to produce low-loss parabolic index optical fibers. This work was a continuation of work done under Contracts Nos. N00019-76-C-0083 and N00019-75-C-0074, under which much of the theoretical and preliminary experimental work was done. The concluding work under these contracts consisted of the following:

(1) Put into operation experimental profiling procedures to test the theory developed under contract N00019-76-C-0083.

DD FORM 1 JAN 73 1473 EDITION OF 1 NOV 65 IS OBSOLETE

→ next page

Unclassified 404 951

SECURITY CLASSIFICATION OF THIS PAGE (When Data Entered)

20. (ii) Institute a program for the measurement and characterization of measured index profiles in preforms and fibers in order to determine the modifications needed in part (i) above.

(iii) Measure physical properties of cesium nitrate solutions for a precise control of unstuffing bath concentration and its variation in time. and

(iv) Measurement of attenuation, dispersion, bending and scattering losses in our fibers.

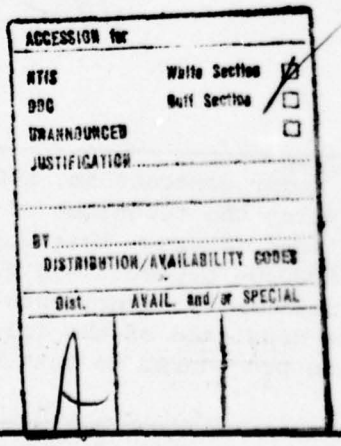

The Catholic University of America

Washington, DC 20064

DEVELOPMENT OF A LOW LOSS OPTICAL FIBER WITH A PARABOLIC PROFILE

by

Vitreous State Laboratory

The Catholic University of America

Washington, DC 20064

FINAL REPORT

Contract No. N00019-76-C-0674

submitted to

NAVAL AIR SYSTEMS COMMAND

Washington, DC 20361

November 1977

TABLE OF CONTENTS

I. Introduction

This is the final report of work completed under contract No. N00019-76-C-0674. The objective of this contract was to develop the technique of Molecular Stuffing to produce low-loss parabolic index optical fibers. This work was a continuation of work done under Contracts Nos. N00019-76-C-0083 and N00019-75-C-0074, under which much of the theoretical and preliminary experimental work was done. The concluding work under these contracts consisted of the following:

(i) Put into operation experimental profiling procedures to test the theory developed under Contract N000-9-76-C-0083.

(ii) Institute a program for the measurement and characterization of measured index profiles in preforms and fibers in order to determine the modifications needed in Part (i) above.

(iii) Measure physical properties of cesium nitrate solutions for a precise control of unstuffing bath concentration and its variation in time.

(iv) Measurement of attenuation, dispersion, bending and scattering losses in our fibers.

II Brief Review of the Molecular Stuffing Process

Molecular Stuffing is based on the Vycor process developed more than forty years ago at Corning but it incorporates a number of important modifications that make the process suitable for optical fiber applications. The process utilizes thermodynamic and chemical properties to produce a high purity glass preform with a controlled index profile. Preforms have been made by Molecular Stuffing that yielded fibers with optical attenuation

less than 10 dB/km and fibers having a graded index profile.

The basic steps in the process are illustrated by the flow diagram shown in Figure 1.

A. Glass Melting

An alkali-borosilicate glass is melted in a conventional resistance heated furnace in a platinum crucible. The batch materials are reagent or high purity commercial grade materials which have transition metal impurities of less than 1 ppm and costing on the order of $1.00/lb in small quantities. The melting and homogenization of the glass can be easily adapted to a 24 hour schedule. After homogenization is complete, the glass is drawn into rods of convenient diameter and is ready for further processing.

B. Phase Separation

The glass rods are placed in annealing furnaces for a specified time at a temperature below the immiscibility temperature of the glass, the exact temperature and time being determined by the composition being used. For the compositions in the range we have examined, a temperature near 500°C and a time of a few hours is appropriate. The purpose of this heat treatment is to obtain a completely interconnected microstructure having a characteristic size of a few hundred angstroms for the phases which consist of an alkali borate phase and one which is more than 90% silica, the remainder being B_2O_3. A fortunate result of the phase separation is that the ionic impurities which include the transition metals

tend to segregate into the alkali borate phase. This facilitates their removal and the purification accomplished in the next step of the process.

C. Leaching

The alkali-borate phase is susceptible to attack by weak acid solutions such as HCl while the silica-rich phase is not. If the proper interconnected microstructure has been obtained in the previous step, leaching for a time on the order of one day will yield a high silica porous structure free of transition metal impurities. This porous structure is then further cleansed of leaching products and acid by washing in filtered, deionized water.

D. Dopant Purification

Cesium nitrate is available from a number of suppliers with transition metal impurities ranging from tens of ppm to a few ppb. A number of standard techniques are available for in-house purification of cesium nitrate including: recrystallization, liquid-liquid extraction, mercury hydrolysis, filtration and ion exchange. As reported in the Quarterly Report under Contract N00019-76-C-0083 dated July, 1976, both recrystallization and/or liquid-liquid extraction performed on Kawecki-Berylco cesium nitrate provides sufficient purification to obtain doped fibers with losses less than 20 dB/km. Combinations of the above techniques are capable of producing cesium nitrate as pure as that obtainable from Merck which is in the ppb range for both iron and copper. This purity level should be sufficient to yield fiber attenuations below 5 dB/km.

E. Profiling

The porous silica structure is an ideal host for the deposition of index and/or physical property modifying dopants. The majority of our work has been with cesium nitrate as a dopant. The dopant is dissolved in an aqueous solution and is allowed to diffuse into the porous glass rod. After a few hours the dopant solution is uniformly distributed in the rod. A step index profile can be obtained by first precipitating the cesium nitrate by means of a temperature drop and/or solvent exchange, and then dissolving the cesium nitrate from a cladding layer in the rod. A graded index can be obtained by replacing the dopant solution with solutions having lower concentrations of dopant and allowing diffusion to produce the desired index profile. After the desired profile is obtained, the dopant is precipitated as is done in the case of a step index.

F. Drying and Consolidation

The stuffed profiled rods are dried and consolidated in combustion tubes in which the atmosphere can be controlled. The rods are slowly heated first to drive off water vapor, and then, as the temperature is raised, the cesium nitrate decomposes, giving off nitrous oxide and is oxidized to cesium oxide. Final drying and the oxidation of remaining iron impurities is accomplished by passing dry oxygen over the rods at about 1/5th of an atmosphere pressure. The temperature of the rods is gradually raised until the rod is fully collapsed at about 850°C. The rod preform is then ready for fiber drawing.

III Diffusion Theory for Dopant Solutions in Porous Preforms

Under Contract N00019-76-C-0083 a theory was developed for the diffusion of dopant solutions in a porous rod. It was shown that by an appropriate choice of boundary conditions one could produce a parabolic dopant profile in porous glass rods resulting in a parabolic index profile in the final glass. The details of this theory are given in the final report of the above contract and are summarized below.

The diffusion equation to be solved is

$$\frac{\partial C}{\partial t} = D\left[\frac{\partial^2 C}{\partial r^2} + \frac{1}{r}\ \frac{\partial C}{\partial r}\right]$$

where $C = C(r,t)$ is the dopant concentration as a function of radial position and time and D is the constant diffusion coefficient.

For the cylindrical geometry of a rod preform and boundary conditions consisting of a step change in dopant concentration at the rod surface followed by a ramp decrease in concentration to zero the solution to the equation can be expressed as an infinite series:

$$C(r,t_f) = \Delta C(1-x^2) + \sum_{n=1}^{\infty} \frac{8\ J_0(\beta_n x)}{\beta_n{}^3 J_1(\beta_n)}\ [\beta_n - \Delta C]$$

where

$$\phi_n = \frac{e^{-\beta_n{}^2 \tau_f}}{4}\ [\theta\ e^{\beta^2 n \tau f} - e^{\beta^2 n \tau 1} + \beta_n{}^2 (C_0 - C_1)]$$

$x = \frac{r}{b}$ where b is the radius of the rod;

$J_0 = (\beta_n) = 0$, J_0, J_1 are Bessel functions of zero and first order;

$$\tau = \frac{Dt}{b^2},\ \theta \equiv \frac{C_1}{\tau_f - \tau_1}$$

$$\Delta C = \sum_{n=1}^{\infty} \frac{8\ \phi_n}{\beta_n{}^3\ J_1(\beta_n)}$$

similar solutions are obtained for single or multiple step changes in concentration with time.

Depending on the choice of boundary conditions it has been demonstrated by computer calculation that one can obtain a composition profile whose standard deviation from a parabola is less than 10^{-8} for the case of a step change followed by a ramp. For a single step the standard deviation can be as small as 10^{-2} and for a double step as small as 10^{-3}. This precision also applies for profiles which represent small deviations from parabolic which may be required to minimize dispersion in optical waveguides.

IV. Profiling Experiments

During this contract period, there was a major effort to produce the profiles predicted for the stuffing process by our diffusion theory. Our preliminary results showed that although graded index profiles could be achieved, the results were not as predicted. It soon became clear that variables not accounted for in the theory must be playing an important role in obtaining the final profile.

A major difficulty in determining the parameters neglected in the theory is the fact that the only step in the process at which the dopant profile may be determined is after the final collapsing. It is thus not possible easily to determine at which stage of the process there is a departure from our predictions. The only path open to us was to complete a large series of experiments systematically varying parameters and looking for an effect on the final product as indicated by the index profile.

For reference, the details of the basic stuffing procedure are outlined below, beginning with the leached porous rod.

1. The porous rod is soaked for three hours in an aqueous solution of approximately 66% cesium nitrate by weight at a temperature near 100°C.

2. Unstuffing is accomplished by replacing the stuffing solution with 98°C flowing water for 7 to 9 minutes depending on the diameter of the rod and as required by the diffusion equations.

3. After unstuffing, the flowing hot water is replaced by flowing cold water ($T \simeq 0°C$) for 20 to 30 seconds.

4. Precipitation is achieved by flushing the cold water out with methanol at 3 or 4°C, followed by a soak for 6 to 15 hours.

5. The rod is dried and collapsed as indicated earlier.

The index profile obtained during one of the first tests of this procedure is shown in Figure 2. Although the profile is graded, there are several serious departures from the predicted profile. The profile is skewed and not centered on the rod axis. The top of the profile is flat and the index at the edge of the rod is much higher than it should be. This type of profile was typical of the early results, although the above mentioned flaws could be present in varying intensity. Some of the resultant profiles ended up more like a step index than a graded index, as seen in Figure 3, for example.

The early results seemed to indicate that some variable or set of variables present in differing degrees in the rods seriously affected the diffusion process. It was thought that something was causing the diffusion coefficient to be smaller near the surface of the rods than it was in the center. This would explain the high index near the edge as well as the poor shape of the profile. Possible sources of such a problem were identified and a series of experiments performed to eliminate them. The experiments attempted are first identified and then explained in detail below.

1. The rods were centerless ground after heat treatment to remove any effect of surface composition difference and to provide a perfectly cylindrical geometry.

2. The porous rods were given a 5% HF wash for 2 to 5 minutes to dissolve anything that might be clogging the pores near the surface.

3. The porous rods were washed with a .5 N NaOH solution for 15 to 90 minutes for the reason stated in No. 2 above.

4. It was found that silica gel formed in the leaching process could be removed by washing the porous rods in 95°C water for 10 days. It was thought that the silica gel might clog the pores.

5. Several sources of cesium were used for stuffing. It was thought that some impurity in the dopant which was not measured at the time (such as silica) could clog the pores.

6. The homogeneity of the base glass was improved to eliminate the possibility of a variation in the microstructure due to inhomogeneity.

A. Centerless Grinding

In the rod forming process, the rod is drawn from the melt with the surface of the rod being drawn from the top layer of glass in the melting pot. This surface layer can be deficient in alkali and borate due to volatilization. This could effect the microstructure near the surface resulting in a diffusion barrier there. A large number of rods were centerless ground to remove the surface layer and to remove any effects that an oval rod might produce. The grinding was done after the phase separating heat treatment.

Aside from the elimination of the obvious effects due to oval rods, the grinding of the preforms seemed to have had no effect. Figures 3 and 4 show two ground rods prepared in a similar manner, yet yielding very different results. The rod in Figure 3 shows a very flat top and the index at the edge is greater than 1.47 (it

should be 1.458). The rod in Figure 4 shows more curvature at the top and has a lower index at the sides. These experiments were repeated several times with similar inconclusive results.

B. HF Wash

It was thought that during the leaching or washing processes something might cause the surface pores to shrink or become clogged with the result that diffusion at the surface would be restricted. A short (2 to 5 minute) wash with a 5% HF solution would allow the pores near the surface to be enlarged without affecting the central pores. A number of rods were treated in this way with varying re-results.

One of the best profiles that we have obtained was made from a rod having the HF wash. The profile is shown in Figure 5. A least squares fit to the central 75% of the rod shows a relative standard deviation from a parabola of about 4%. A second rod shown in Figure 6 was given an identical treatment. This profile is almost a step profile. Although the HF wash may help in some cases, it is not the controlling factor since we were not able to reproduce the results shown in Figure 5 with any consistancy.

C. NaOH Wash

For the same reasons as given above for the HF wash, a .5 N NaOH wash was tried. This procedure never gave good results. A typical profile using this procedure is shown in Figure 7.

D. Hot Water Wash

It is known that silica gel is formed in the leaching process. This gel is deposited in the pores and reduces their ef-

fective size thus affecting the diffusion of dopant in the rods. The silica gel may be removed by washing the rods for approximately 10 days in water at 95°C. The removal of the silica gel can be observed by monitoring the weight of the porous rod. The dissolution of the gel proceeds at a much greater rate than the attack and dissolution of the silica skeleton, so it is clear when removal is achieved.

As in the other experiments,no positive correlation between profile quality and silica gel removal was seen. Figure 8 shows a typical profile achieved. The top is too flat and the edges are too high.

E. Dopant Purity

The purity of the dopant, cesium nitrate, in these experiment varied considerably. It was thought that some contaminant might exist which could affect the diffusion process. Experiments were performed with commercial high purity cesium nitrate from Kawecki Berylco, with ultra-pure cesium nitrate from Merck and with cesium nitrate purified in our own laboratory. Figures 9 and 10 show almost identical profiles which were obtained from Merck and Kawecki Berylco cesium nitrate respectively. The dopants were very different in purity, the Merck having measured transition metal impurities in the ppb range and Kawecki Berylco in the ppm range. It is possible that all cesium samples tested had some unmeasured impurity such as silica but the results of many experiments did not indicate that the source of dopant had any effect on the final profile.

F. Homogeneity

In the early experiments the optical quality and thus the compositional homogeneity were not very good. In particular, visible striae were present in the rods due to incomplete mixing and due to the folding-in of alkali-poor surface layers as the batch glass was stirred. Since the striae represented a slightly different composition from the average, the pores in that region would be a different size. This would affect both the diffusion and the amount of dopant deposited in these pores. Interferograms showed that these striae persisted throughout the process and could be observed in the final glass.

Stuffing experiments were performed on glass having both good and poor homogeneity. The result was that although the striae affected the local index, they had very little influence on the general shape of the profile. Figure 5 has a good profile but the interferogram in Figure 11 shows the presence of striae which distorts the interference pattern. Figure 12 , however, shows a poor index profile while the interferogram is relatively free of striae as seen in Figure 13 . Homogeneity of the base glass does not appear to be the controlling factor in profile control.

The result of the stuffing experiments has been that it is possible to obtain a very nearly parabolic profile by molecular stuffing as predicted. It is clear however that some parameter or set of parameters not included in the theory may have a strong influence on the profile. These parameters do not appear to be

among the parameters we have discussed above. One of the few clues to come out of this work was the observation that the profiles produced using certain batches were consistently better than those produced from other batches. Batches having almost identical analyzed composition, coexistence temperature and other physical parameters simply did not have the same stuffing characteristics. At the present time we do not have an answer to the problems of controlling the profile adequately and consistently. Work is being continued in this area with support from private industry.

V Profile Measurements

A. Refractive Index Profile Measurements

Because of differing requirements at several stages of this project it was necessary to develop three techniques for measuring index profiles in fibers and in preforms. Crude but quick measurements can be made on the preforms by measuring the angular deviation of a laser beam passing through a prism made from the preform. More accurate measurements can be made on the preforms using a Michelson interferometer operated in the Twyman-Green mode, i.e., parallel illumination. The most accurate way of measuring the index profiles in fibers is the interference method using an interference microscope. Because of limited resources, however, we chose the much simpler and less costly technique of measuring the near field intensity distribution which is related to the index profile.

In our initial experiments we were interested in obtaining quick, moderately accurate measurements of the preform profiles. A simple way of doing this is to measure the deviation of a laser

beam passing through the apex of a prism made from the preform. The prism geometry is shown in Figure 14 and a schematic of the measuring apparatus is shown in Figure 15.

The procedure for sample preparation and measurement is relatively simple. A 90° prism angle is ground from the cylindrical preform with the angle bisected by the axis of the cylinder. A surface obtained by a final grind with #600 grit metallurgical grinding paper is sufficient. The sample is placed with its axis vertical in the sample cell which has been filled with paraffin oil (n = 1.471). A weakly focused laser beam (diameter =.1 mm) passes partly through the apex of the prism and partly through the paraffin oil alone. A zero reading is obtained on the micrometer by rotating the mirror until the beam passing through the oil alone is reflected back on itself as observed by the spot appearing on the focusing lens. The beam passing through the prism is then made to retrace its path by further rotating the mirror clockwise or counter-clockwise depending on whether the glass index is above or below that of the paraffin oil. This procedure is repeated for various positions on the radius of the preform to obtain the deviation angle δ as a function of radial position.

The prism deviation angle can be related to the refractive index of the prism and the surrounding medium using geometrical optics. Solving for δ one obtains:

$$\delta = \phi_1 - \alpha + \sin^{-1}\frac{n'}{n}\{\sin[\alpha - \sin^{-1}(\frac{n}{n'}\sin\phi_1)]\}$$

where the angles are defined in Figure 14 and n and n' are the index of paraffin oil and the glass respectively. For the case

of a 90° prism angle and a 45° angle of incidence we have the following simple relation:

$$n' = n\sqrt{\sin^2\left(\delta + \frac{\pi}{4}\right) + .5}$$

The accuracy of these measurements was estimated to be better than ± 0.0005 for an index near 1.47, the chief source of error being the accuracy with which one could judge the moment when the laser beam was retracing its path. This estimate of the accuracy was confirmed by comparison of index measurements made on our samples in our and in another laboratory (American Cystoscope Makers, Inc., of Stamford, Connecticut).

For making precise observations of the variation in index in a cross-section of a preform, a Twyman-Green interferometer can be used. A schematic of the interferometer is shown in Figure 16. The plates of the interferometer are adjusted to give an interference pattern in the viewing plane. The sample is placed in the path between the beamsplitter and one of the mirrors. The observed deviations in the interference pattern are due to the additional optical pathlength in the sample. A sample having accurately ground and polished flat faces and a uniform index will give an interference pattern as shown in Figure 17 which is the photograph of the interference pattern from a homogeneous piece of the untreated base glass. Figures 11 and 13 show the interference patterns obtained from graded index Molecular Stuffed samples. The first of these shows a great deal of inhomogeneity in the index profile due to striae existing in the base glass prior to processing. The second of these shows a much more uniform profile

but there is still some evidence of inhomogeneity near the center of the sample. Although quantitative results can be obtained from the interferograms, we have only used them for qualitative observations to date.

B. Fiber Index Profile Measurements

Because of the small diameter of the fibers (175μ or less) it is difficult to make direct index measurements. Although interference microscopes exist which will measure index variations in small samples, these instruments are costly and there were not any available to our laboratory. An indirect technique of measurement is possible which consists of measuring the near field intensity profile in a fiber for which all modes are equally excited with the exception of leaky modes. It has been shown[1] that the near field intensity profile is related to the index profile according to the relation:

$$\frac{P(r)}{P(o)} = \frac{n^2(r) - n^2(2)}{n^2(0) - n^2(2)}$$

where P(o) and P(r) is the intensity at the fiber center and at position r respectively; n(0), n(2) and n(r) are the indexes at the center, in the clad, and at position r respectively.

The apparatus for measuring the near field intensity profile of a fiber is shown schematically in Figure 18. A measurement is made simply by exciting the modes of a fiber with an incoherent source, projecting the image of the flat output end of the fiber and scanning in the image plane with a detector having

a small aperture. The difficulty in such a measurement is insuring that all ordinary modes are equally excited and that the leaky modes are not present. By making measurements using fibers of different lengths, one can determine a length suitable for attenuating the lossy, leaky modes while not losing appreciable power from the propagating, higher order modes. For our fibers, one or two meters is usually sufficient for measurment. Figure 19 shows index profiles measured on a preform and a fiber drawn from that preform. The observed differences may be real or could be due to errors in the preform measurement. The steep portion of the step profile is difficult to measure accurately with the prism method. It would be useful, however, to confirm the results by comparison with results from an interference measurement.

VI. Physical Property Measurement for Unstuffing Bath Concentration Control

The computer studies of the stuffing procedure indicated that a few step changes in stuffing concentration with time would be sufficient to acheive a parabolic index profile with a standard deviation of less than .1% in index. The saturation concentrations of cesium nitrate in several solvents as a function of temperature give a sufficient range of concentrations to obtain the desired profile control. These solubilities were measured for a number of solvents and the results are shown in Figure 20. By controlling the temperature of the dopant solution the concentration is conveniently controlled.

VII. Fiber Propagation Characteristics

A. Rayleigh Scattering

An upper limit to the Rayleigh scattering in both bulk glass and fibers may be obtained by performing a Landau-Placzek scattering measurement at a scattering angle of 90°. This technique, combined with a measurement of total scattering and the angular scattering distribution, is useful in separating contributions to scattering from Rayleigh scatterers, which are related to intrinsic bulk properties, and scattering from core diameter perturbations and/or needle-like scattering particles. Since most of the Rayleigh scattering is related to intrinsic bulk properties of the glass, it represents a lower limit to the attenuation.

The measurement of Landau-Placzek ratios in glasses has been described thoroughly in the literature.[2,3] Briefly, the light scattered by the glass from a collimated laser beam is collected at a convenient scattering angle such as 90°. The light is frequency analyzed by a scanning Fabry-Perot interferometer which resolves the unshifted Rayleigh line and the Brillouin lines which are shifted upward and downward in frequency due to scattering from acoustic waves. A schematic of a typical experimental setup is shown in Figure 21. . The Brillouin intensities are a weak function of the glass composition, while the Rayleigh scattering is a function of both composition and thermal history of the glass. The absolute Brillouin intensity can be calculated if the stress optical coefficients are known for the glass of interest. The Brillouin intensities can then be used as a calibration for estimating the Rayleigh intensity. If the coefficients

are not known, a less accurate result may be obtained by using a measurement of a known glass such as fused silica to calibrate the sample measurement. The latter technique was used to measure the upper limit of the intrinsic scattering in both preform and fiber samples of Molecularly Stuffed glass.

The scattering attenuation is given by

$$\alpha_s^{(1)} = \alpha_s^{(2)} \frac{I_B^{(1)}}{I_B^{(2)}} \left(\frac{1 + R_{LP}^{(1)}}{1 + R_{LP}^{(2)}}\right)$$

where $\alpha_s^{(1)}$, $\alpha_s^{(2)}$, are the scattering attenuation of the sample and of fused silica respectively; $I_B^{(1)}$, $I_B^{(2)}$ are the Brillouin intensities of the sample and fused silica and $R_{LP}^{(1)}$, $R_{LP}^{(2)}$ are the Landau-Placzek ratios of the sample and fused silica respectively where the Landau-Placzek ratio is defined by $R_{LP} = I_R/2I_B$. $\alpha_s^{(2)}$ is known and is approximately 1 dB/km at 0.85μ.

Measurements performed on Suprasil II fused silica and cesium doped Molecular Stuffed preforms indicated a scattering loss for the Molecular Stuffed preform of approximately 2 dB/km at .85μ. Measurements performed on fibers involve a slight complication due to the fact that the large numerical aperture of the fibers means that light collected at 90° from the fiber axis and beam direction may actually be scattered at a range of angles. This is due to the fact that if all of the fiber modes are excited, then light is propagating in the fiber at all angles allowed within the NA of the fibers. This results in a broadening

of the Brillouin peaks and one must be careful to use the integrated Brillouin intensities in calculating the Landau-Placzek ratios. Also,because of the small size of the fiber, it is difficult to avoid collecting light scattered from the fiber surface. This may be minimized by carefully stripping the cladding modes from the fiber with a suitable mode stripper. Measurements made on a Molecularly Stuffed fiber indicated a loss of approximately 2.5 dB/km which is in reasonable agreement with the bulk measurement considering the uncertainties in the measurement.

B. Total Light Scattering Measurements

In addition to Rayleigh scattering, fibers may exhibit significant scattering due to a variety of particles or local dielectric variations present in the fiber. In this case a scattering measurement at one scattering angle is not sufficient to obtain the total scattering at all angles. An integrating sphere or similar device is required to make such a measurement.

A simple integrating cube was described by Tynes[4] that is very convenient for measuring the total scattering in fibers. This integrating cube is constructed of six matched silicon solar cells. Two opposing faces of the cube have small holes to allow the entrance and exit of the fiber. The cell is filled with an index matching fluid such as glycerin that couples out the light scattered from the core into the clad in the near forward direction. It is thus possible to collect nearly all of the light scattered from the core with the exception of that striking small dead areas in the cube near the edges and near the fiber entrance and exit holes.

A schematic of the experimental setup is shown in Figure 22. The light from a laser or other bright light source is focused on the end of the fiber. Before entering the scattering cell, the fiber is passed through a tube filled with glycerin to strip out accumulated cladding modes. The fiber is passed through the cell which has a length of 1 cm. The light scattered by the core in that one cm is detected and the resultant signal is read from a voltmeter. The scattering as a function of position in the fiber is measured. Regions of minimum scattering for a good fiber are expected to be representative of the intrinsic Rayleigh scattering while high scattering regions have large contributions from other scattering sources. The absolute scattering attenuation at any point may be determined by first measuring the scattering intensity and then breaking the fiber and using the cell to measure the light being transmitted in the fiber at that point. The scattering attenuation for small scattering is then given simply by

$$\alpha_s(\text{dB/km}) = 10^6 \frac{I_s}{I_o} \log_{10} e$$

where I_s and I_o are the scattered and transmitted intensities respectively.

As a check on the absolute magnitude of the measured scattering intensities a silicone clad Suprasil II fiber with total attenuation at 0.85μ of approximately 20 dB/km was measured. The average scattering loss was approximately 6 dB/km which is the order of magnitude expected for such a fiber. The minimum scattering loss for this fiber was about 3 dB/km which is higher than

the expected intrinsic Rayleigh scattering loss but probably contains excess contributions from the silicone silica interface because of the large NA used in making this scattering measurement.

A molecular stuffed fiber with total attenuation at 0.85μ of approximately 25 dB/km when measured with light launched at 0.07 NA was examined to determine the minimum scattering. Five one-cm-long regions having an average scattering attenuation of 2.7 dB/km measured with a launching NA of 0.09 were found by examining five short sections of fiber chosen at random from the 20-meter-long fiber. A second measurement was made at the same points using a launching NA of 0.18. These measurements indicated an increase in average scattering to a value of 4.2 dB/km. This is probably due to increased scattering from the core clad interface. These low scattering regions were further analyzed with respect to the angular distribution of the scattered light as is described in the next section. The angular distribution found was identical to that expected for Rayleigh scattering. The magnitude of the total scattering is consistent with that found in the Rayleigh-Brillouin measurements reinforcing the conclusion that the intrinsic scattering for these fibers is less than 2.5 dB/km at 0.85μ.

C. Angular Distribution of Scattered Light

The measurement of the angular distribution of the scattered light can be used to obtain information about the nature of the scattering mechanism. Rayleigh scattering from a linearly polarized beam is characterized by a $(1 + \cos^2 \theta)$ angular distribution factor. Both core diameter variations and long dielectric needles

can give rise to a strong forward scattering contribution. Measurements of the angular scattering for fibers was reported by Rawson [5] along with his interpretation identifying both the Rayleigh contribution and contributions from dielectric cylinders.

The angular distribution of scattered light from molecular stuffed fibers was measured. Particular interest was paid to regions identified in the previous total scattering measurements as strong scattering regions and weak scattering regions. A schematic of the experimental setup is shown in Figure 23. The light from a laser was focused on the end of a fiber. The fiber was passed through a cell filled with paraffin oil. The cell was centered on a rotatable table whose angular orientation could be read to one minute of arc. Black paint applied to all but the central one cm of the fiber served both to mask all but that section from the detector optics and stripped accumulated cladding modes. By measuring scattered intensity as a function of the orientation of the fiber with respect to the axis of the collection optics, and making the appropriate corrections for changes in the collection volume with orientation, the angular intensity distribution could be obtained.

It was found that the weak scattering regions had a $(1+\cos^2\theta)$ angular distribution characteristic of Rayleigh scattering. A typical intensity-versus-angle plot for one of these regions is shown in Figure 24. The strong scattering regions however had both the Rayleigh scattering contributions as well as a strong forward scattering contribution which could be orders of magnitude greater than the Rayleigh contribution. A typical angular dis-

tribution for one of the strong scattering regions is shown in Figures 25 and 26.

If the source of the strong forward scattering is assumed to be dielectric cylinders as in the interpretation of Rawson,[5] one can estimate the length of the cylinders from the angular width of the forward scattering peak according to the expression

$$\theta_{1/2} = [.8856\ \lambda\ /(L\eta_o)]^{1/2}$$

where $\theta_{1/2}$ is the angular width at 1/2 maximum, λ is .5145 μ, η_o is 1.47. The index of paraffin oil and L is the length at the scattering cylinders. For the scattering region of Figure 25 the length of the cylinders is estimated to be approximately 250μ. If the cylinders are assumed to be the result of the stretching during fiber drawing of small spherical inhomogeneities existing in the preforms, it is estimated that the diameter of the spheres in the preforms would be approximately .25μ. An examination of the preforms in an electron microscope revealed the presence of spheres approximately .25μ in diameter. The source of these spheres is not known but may be due to silica gel formed during the molecular stuffing process and not fully dissolved in the sintering step or in fiber drawing.

D. Pulse Dispersion Measurements

Due to the fact that the various modes in a multimode fiber do not travel down the fiber with equal velocity, the phenomenon of pulse broadening is observed. If one considers the modes to be represented by rays launched into the fiber at specific angles to the fiber axis, it is easy to see the source of the pulse

broadening. Simply stated, a ray traveling at a small angle with respect to the fiber axis travels a shorter distance than one traveling at a steep angle. The resultant pulse broadening or dispersion can be measured directly by launching a narrow pulse into a fiber and measuring the width of the pulse after passing through a length of fiber.

Apparatus for measuring pulse dispersion was built in our laboratory with a design similar to that described by Andrews.[6] A schematic of the measurement apparatus is shown in Figure 27. The light source is an injection GaAs laser (RCA SG-2001) driven by 5 ampere 5 nsecond pulses at a repetition rate of 2 to 5 kHz. The light pulse (λ=.9μ) is collected by a 20X microscope objective and coupled into the fiber with a 100X objective. The light exiting the fiber is detected by either a PIN or an avalanche silicon photodetector whose output is recorded by a sampling oscilloscope. The triggering of the oscilloscope is delayed with respect to the launched pulse to allow for the transit time of the pulse through the fiber.

Dispersions measurements were made on a 1 km-long step index Molecular Stuffed fiber having an attenuation at .9μ of approximately 20 dB/km. Figure 28 shows the pulse shape after traversing several meters and after traversing 1 km of fiber. The pulse from the short fiber has a width at half maximum of .8 nsec which represents the instrumental width of the system. The pulse from the long fiber is highly asymmetric due the the high attenuation of the higher order modes and has a width of 13 nsec. This implies a bandwidth for the fiber of the order of 70 to 80 Mbits/sec-km.

Molecular Stuffed graded index preforms of sufficient quality and size have not been available for drawing fibers suitable for dispersion measurements. It would be expected that these preforms would give improved bandpass over the step profiled preforms.

CONCLUSION

The purpose of this research was the development of the Molecular Stuffing process to produce low loss optical fibers having a parabolic index profile. The first stage of the research was the development of a diffusion theory applicable to a porous cylinder immersed in a dopant solution. The second stage involved the determination of diffusion coefficients solubilities and related physical parameters needed for application of the theory. The final stage was the production of preforms having parabolic index profiles.

The development of the diffusion theory was very successful. It was discovered that by a series of step changes in dopant concentration with time or by a step change followed by a ramp in concentration one could theoretically obtain a parabolic or if desired, a near-parabolic profile to within a standard deviation of 10^{-8}. This was verified by direct computer calculation.

As a dopant, $CsNO_3$ in aqueous solution proved to have very desirable characteristics. It could be purified relatively easily. It was found that solution concentration could be well controlled by controlling the temperature of a saturated solution. Precipitation and controlled disssolution of the $CsNO_3$ could be obtained by temperature change and the use of organic solvents. $CsNO_3$, which becomes Cs_2O in the final glass also has the index

modifying effects necessary for use in optical fibers. In short, it met all the requirements for use in Molecular Stuffing.

A large number of preforms were produced with varying success. The fact that several profiles were produced with nearly parabolic profiles has convinced us that Molecular Stuffing as it has been developed can be successful. There are however, important effects which are not accounted for in our theories and further work is required to control these effects. This work is continuing with support from private industry and it is expected that the results will be positive.

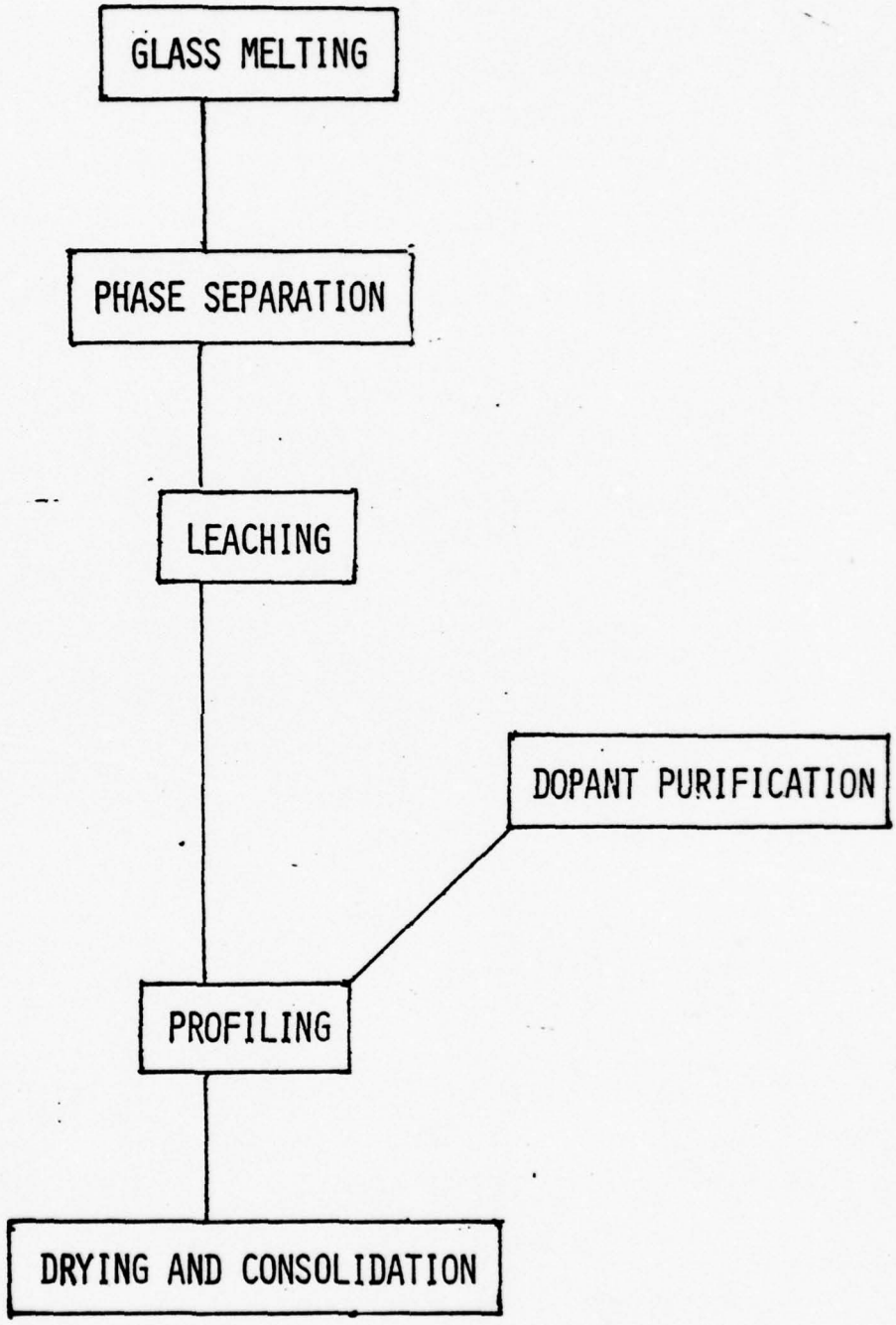

Fig. 1. Flow diagram of the Molecular Stuffing process.

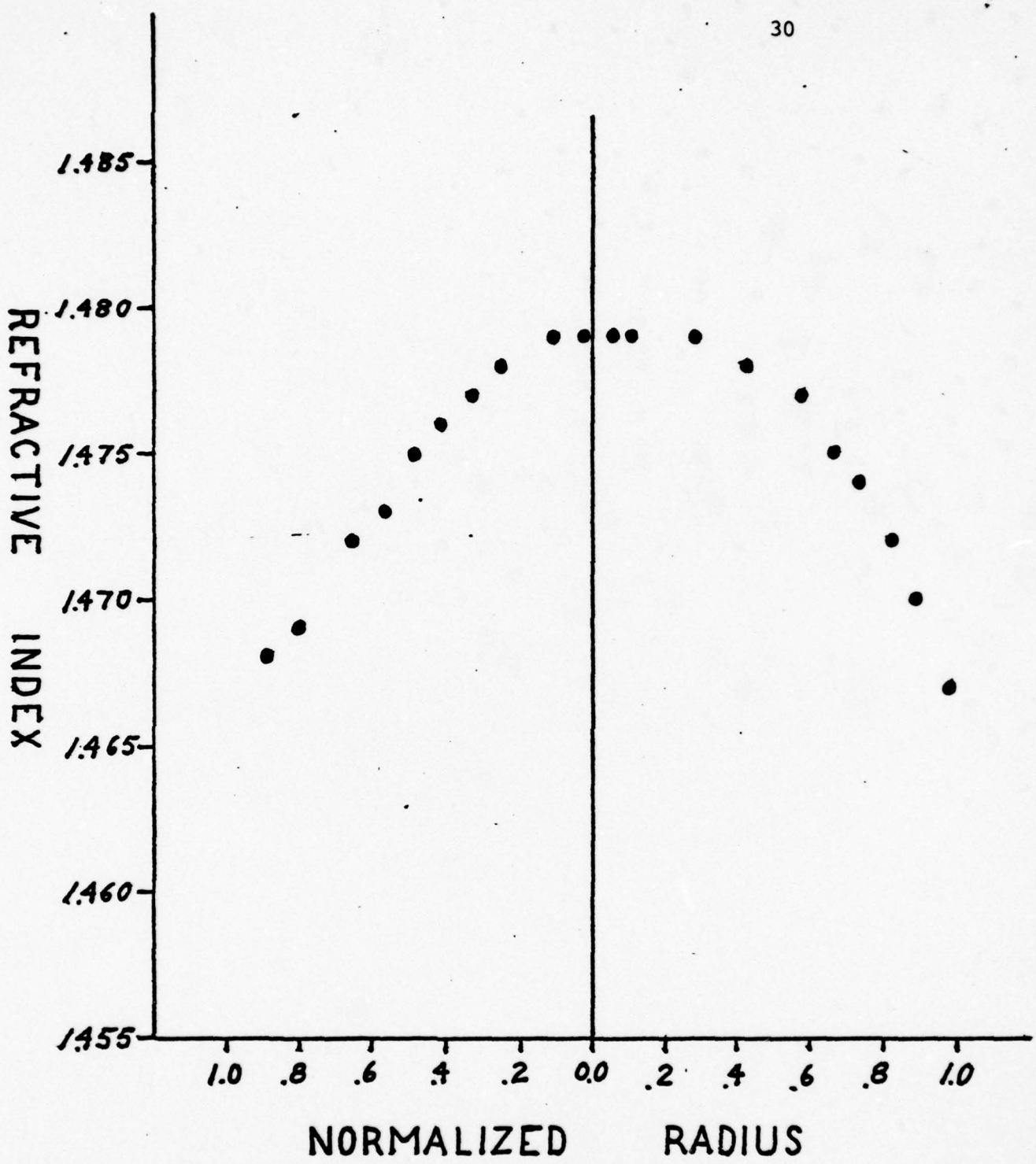

Fig. 2 An early graded index profile showing various profile errors including a flat top, high index at the edges and a skewed profile shape. Rod 2097.

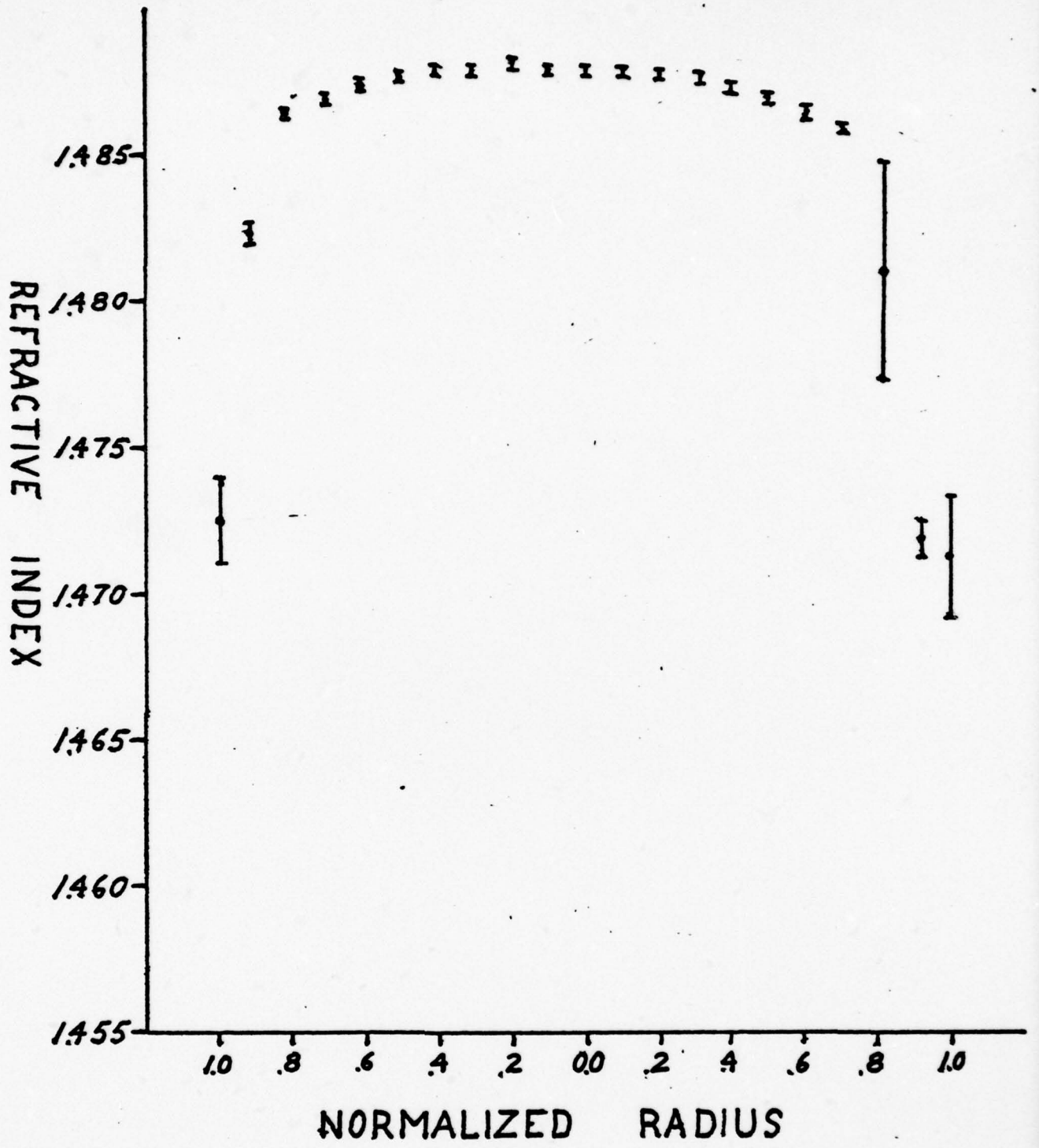

Fig. 3 The index profile in a centerless ground rod showing poor profile results. Rod. 2508.

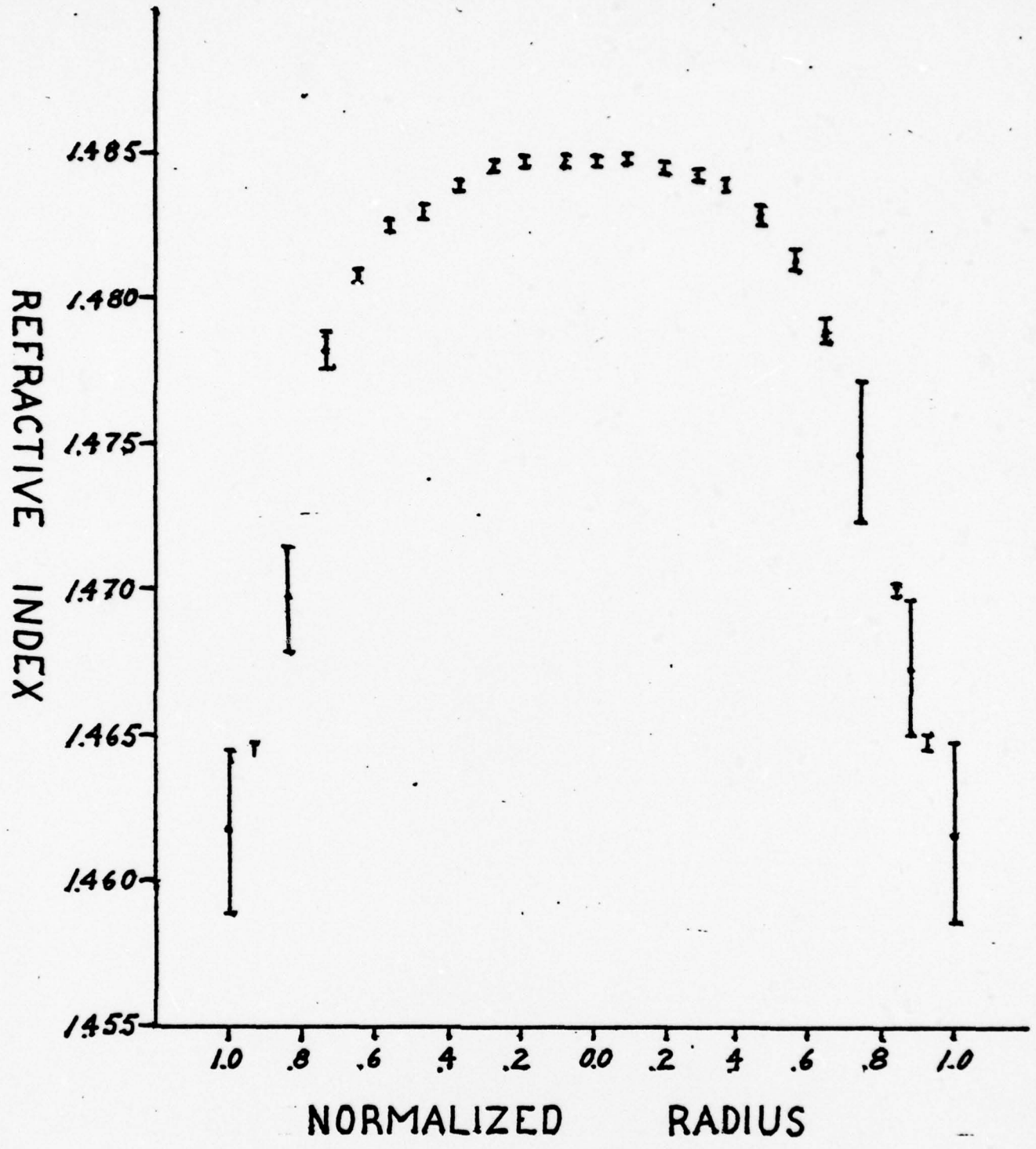

Fig. 4. The index profile of a centerless ground rod showing a moderately good profile. Rod 2510.

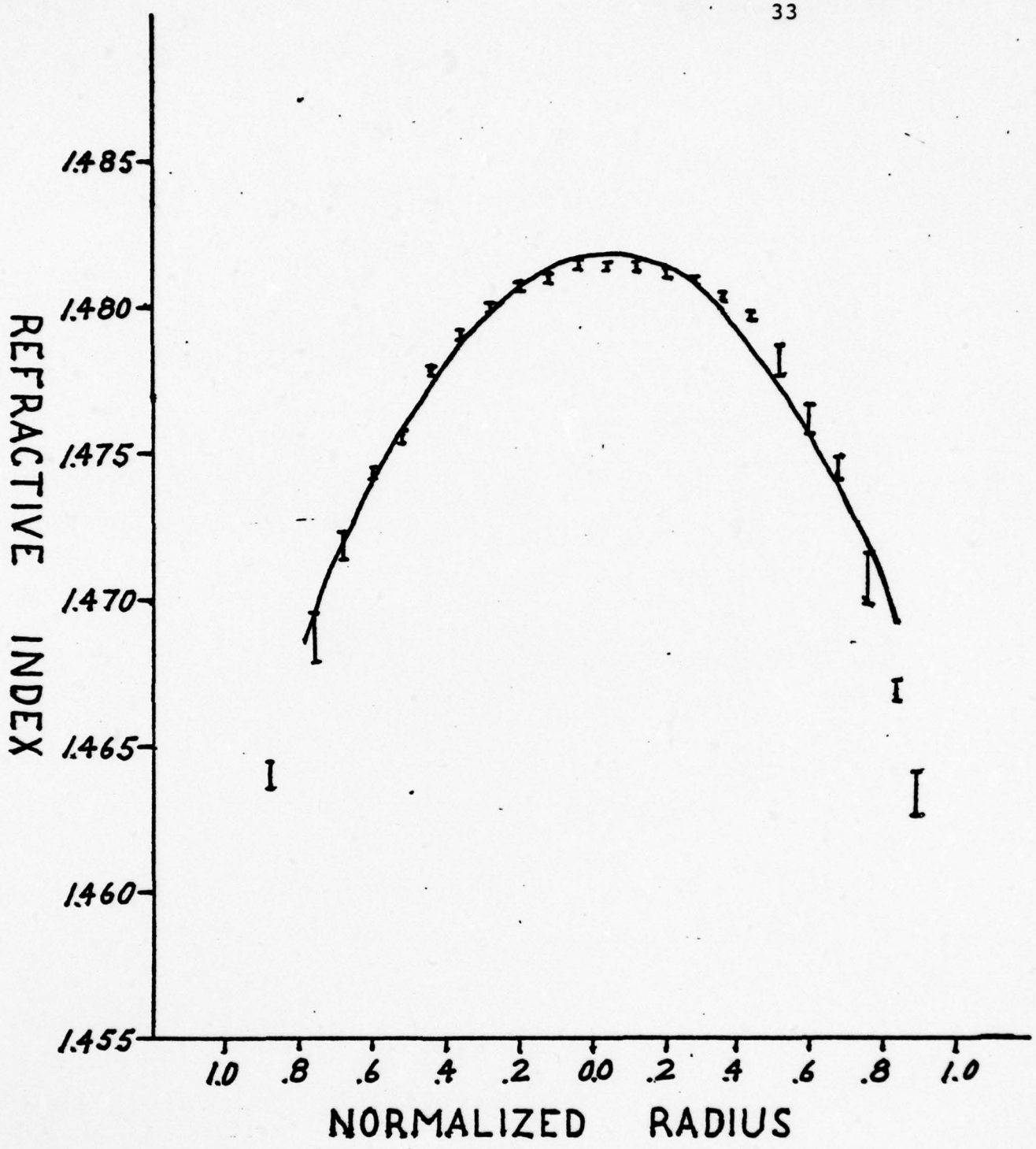

Fig. 5 The profile of a rod given an HF wash. The standard derivation of the data from the parabola shown by the solid line is 4% for the central 75% of the profile. Rod 2518.

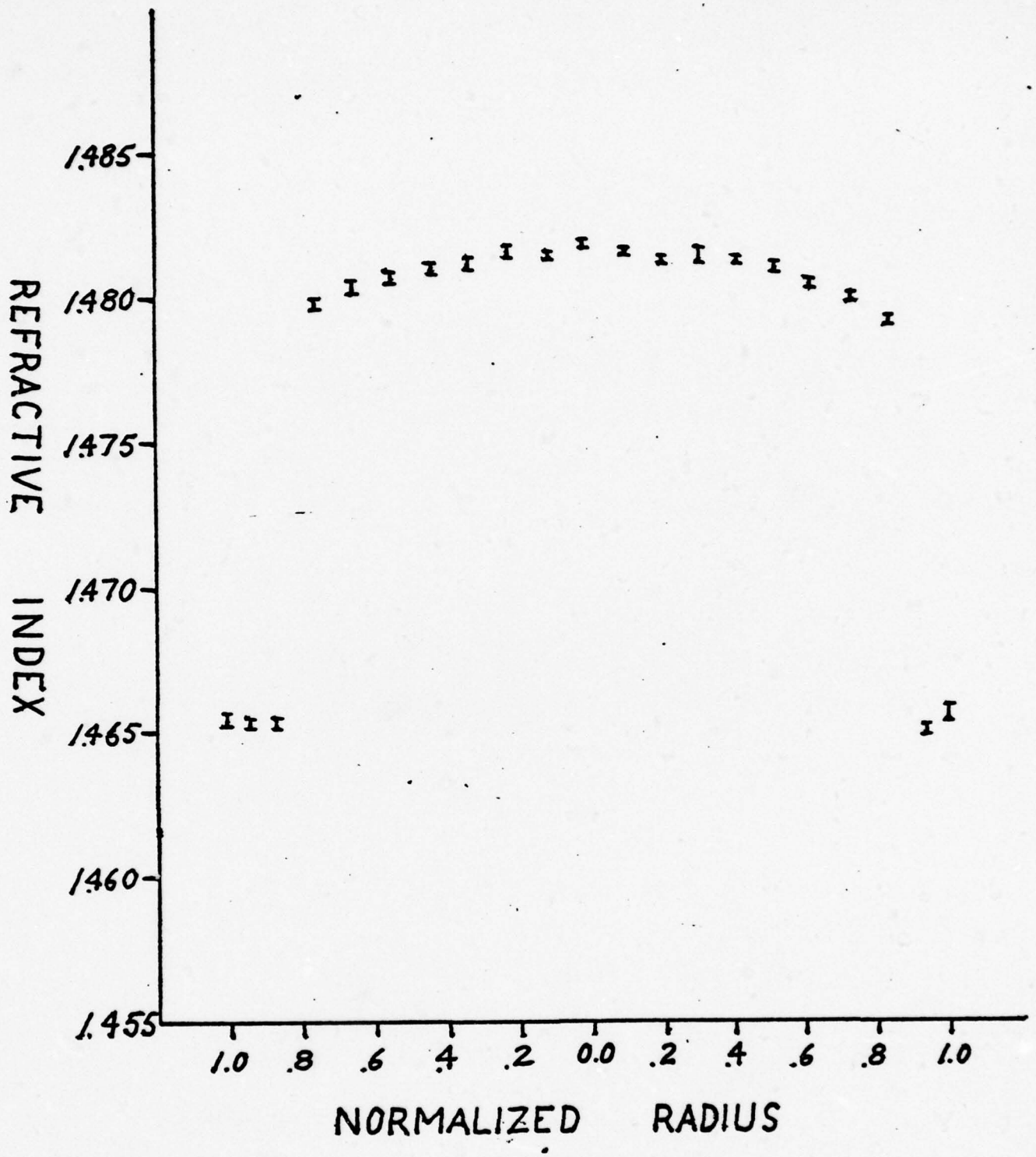

Fig. 6. The profile of a rod given an identical treatment to that of rod 2518. The profile is poor, however, being almost a step profile. Rod 2949.

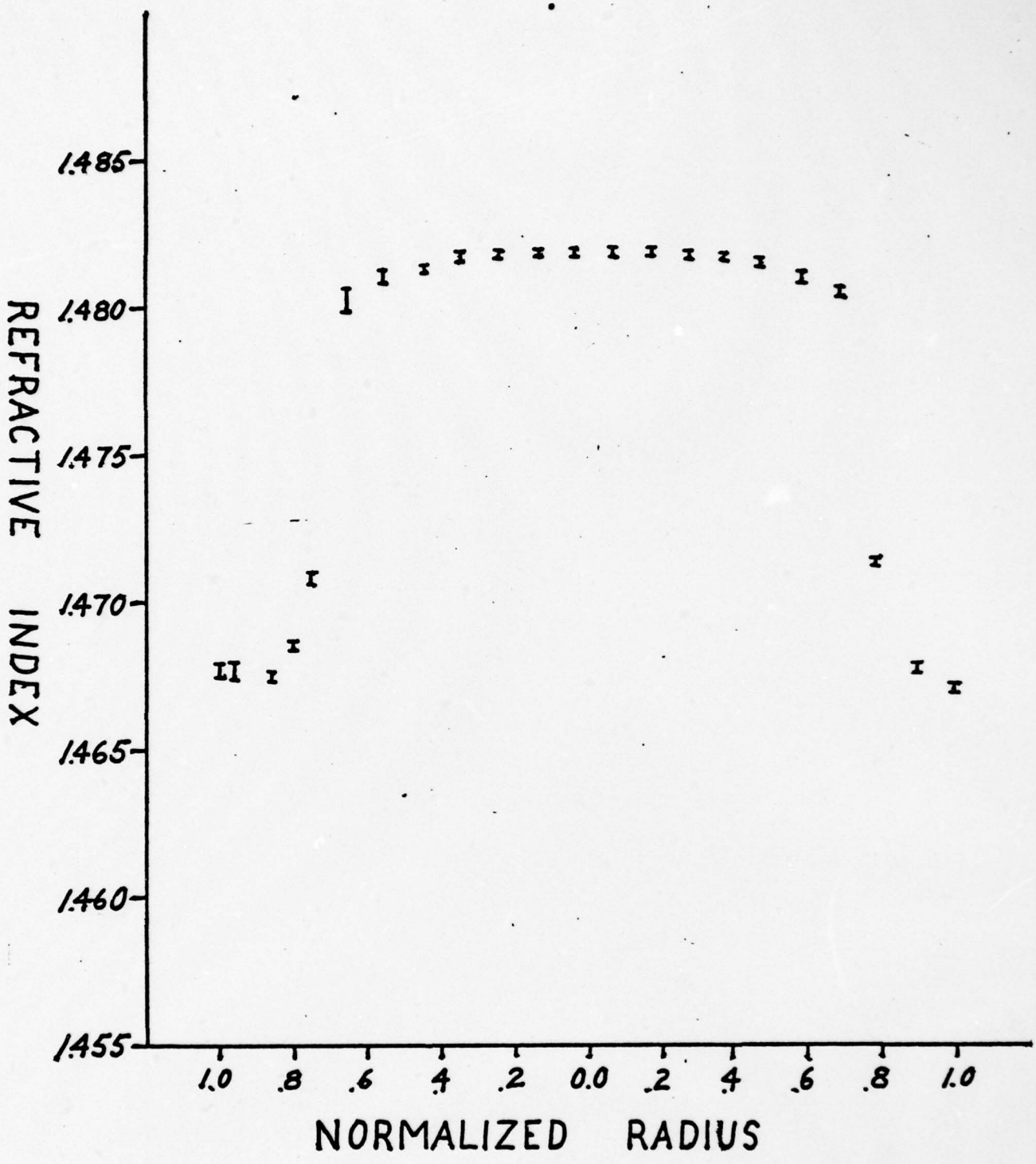

Fig.7. The profile of a rod having a NaOH wash. The profile is poor. Rod 2826.

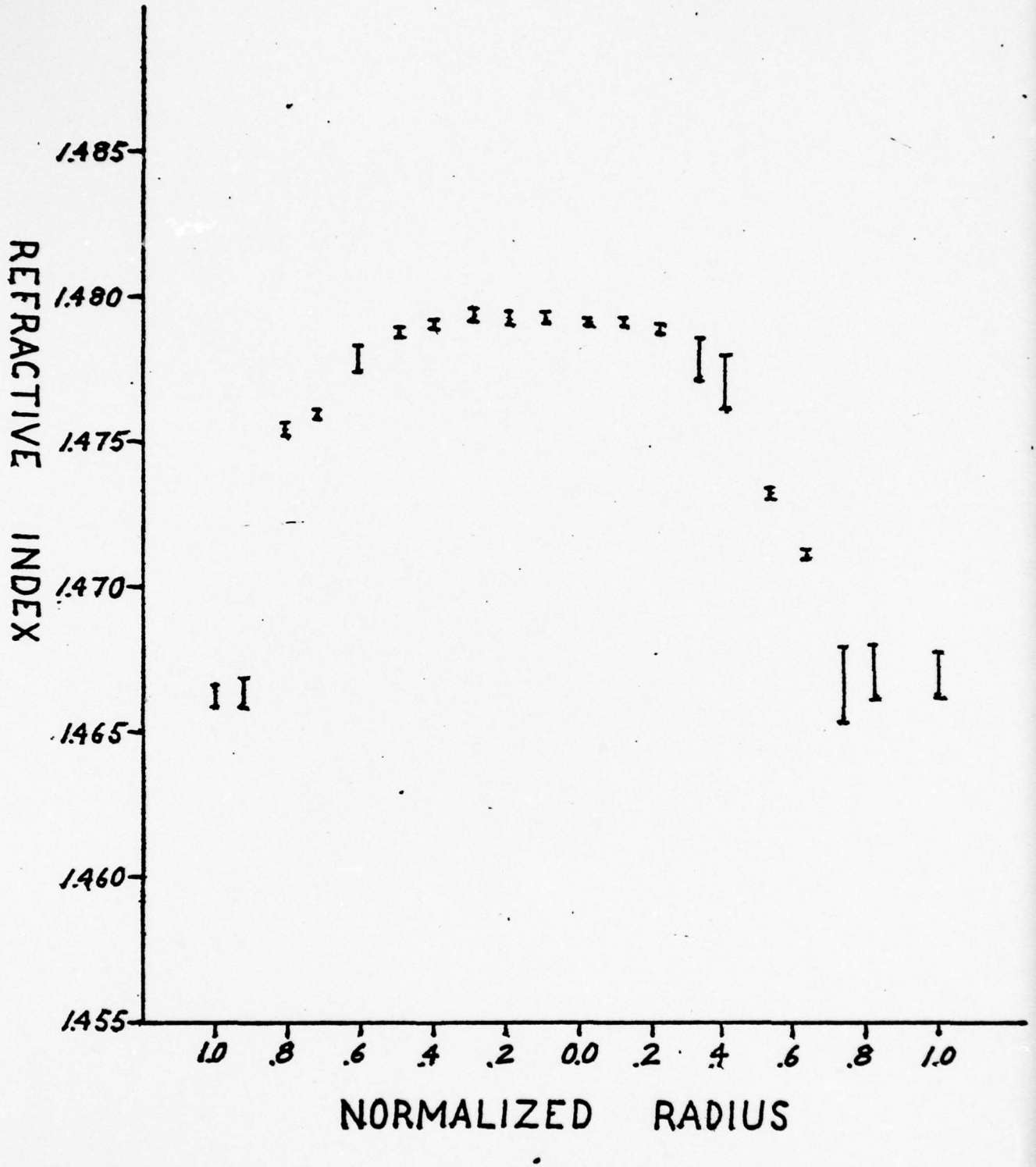

Fig. 8. The profile of a preform prepared from a rod from which the silica gel was removed by a hot water wash. The profile has a flat top and high edges. Rod 2933.

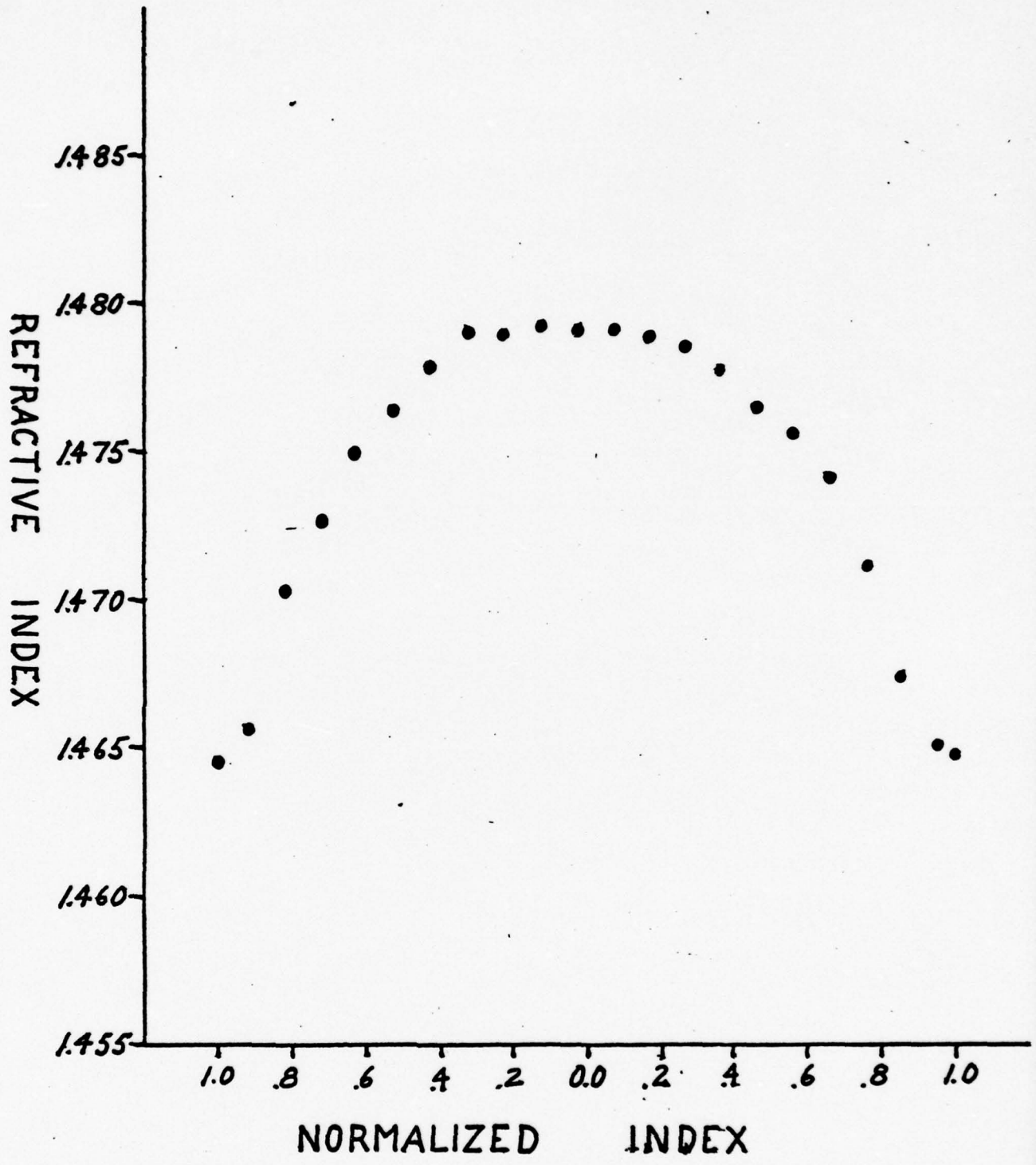

Fig. 9. The profile of a rod doped with Kawecki-Berylco $CsNO_3$. The profile is moderately good in shape but the edges are too high. Rod 2892.

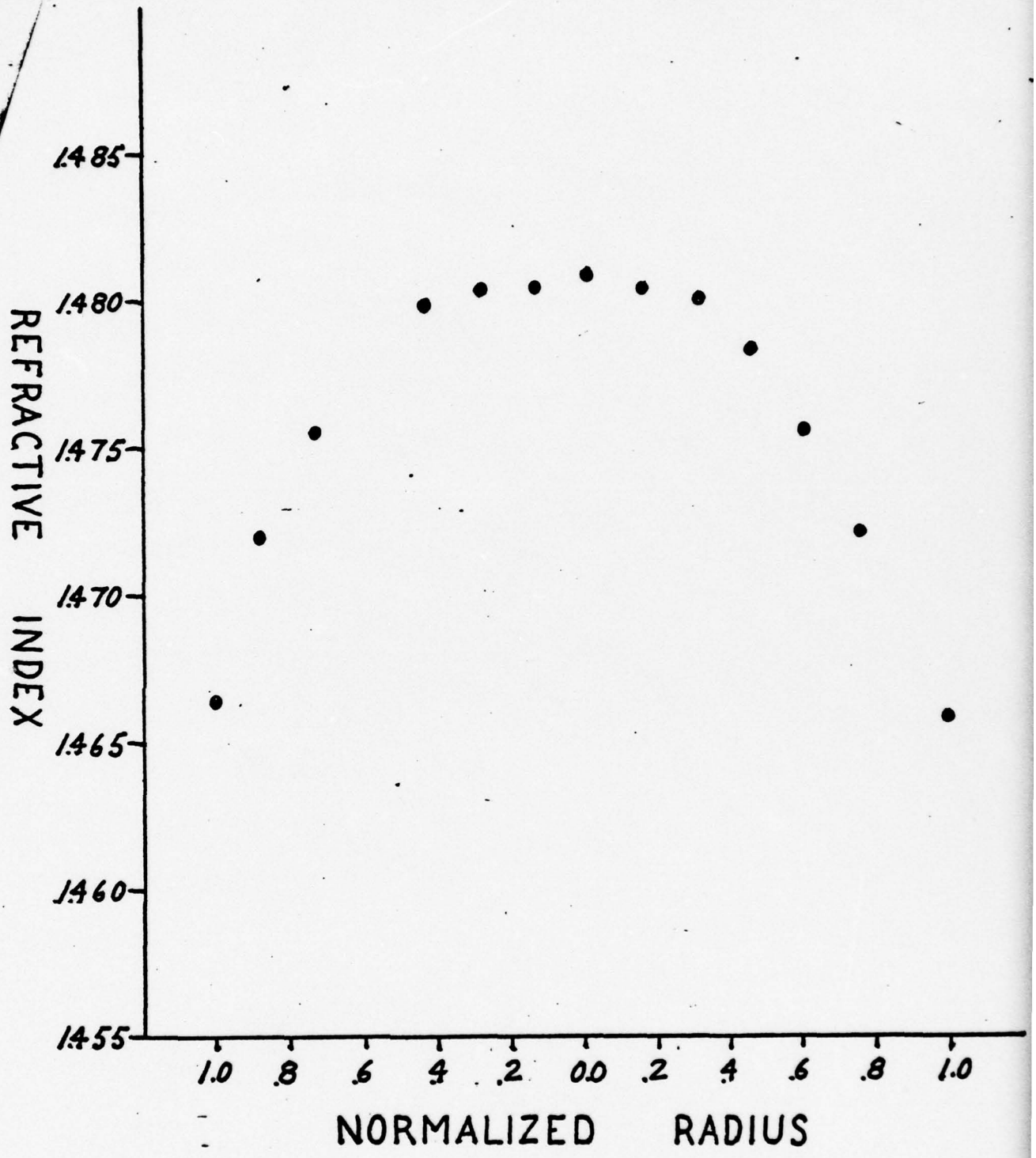

Fig. 10. The profile of a rod doped with ultra-pure $CsNO_3$ from Merck. The profile is nearly identical to that shown in Fig. 9. Rod 2889.

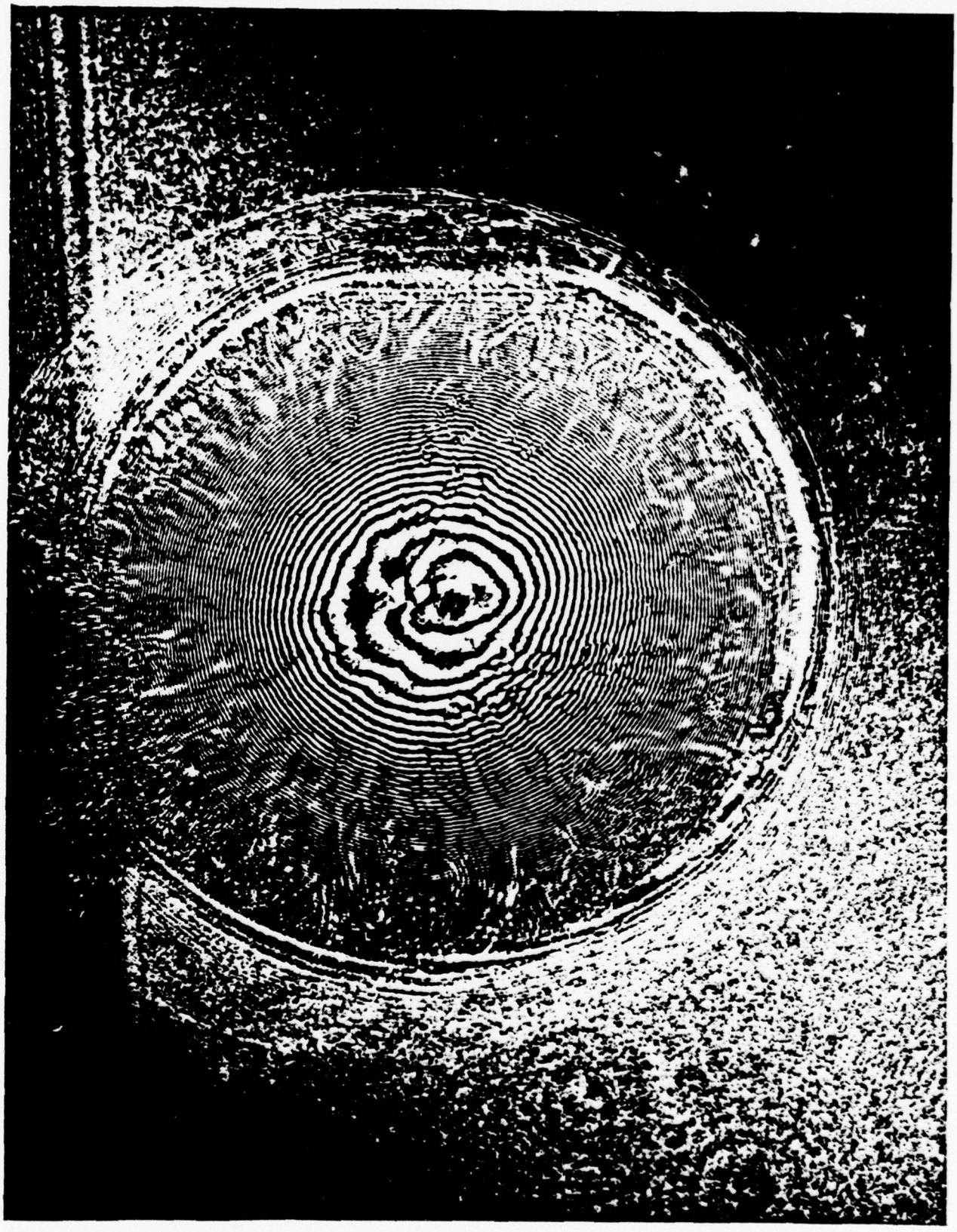

Fig. 11 Interferogram of a rod cross-sectiom having a parabolic profile. General inhomogeneity in the base glass is observed.

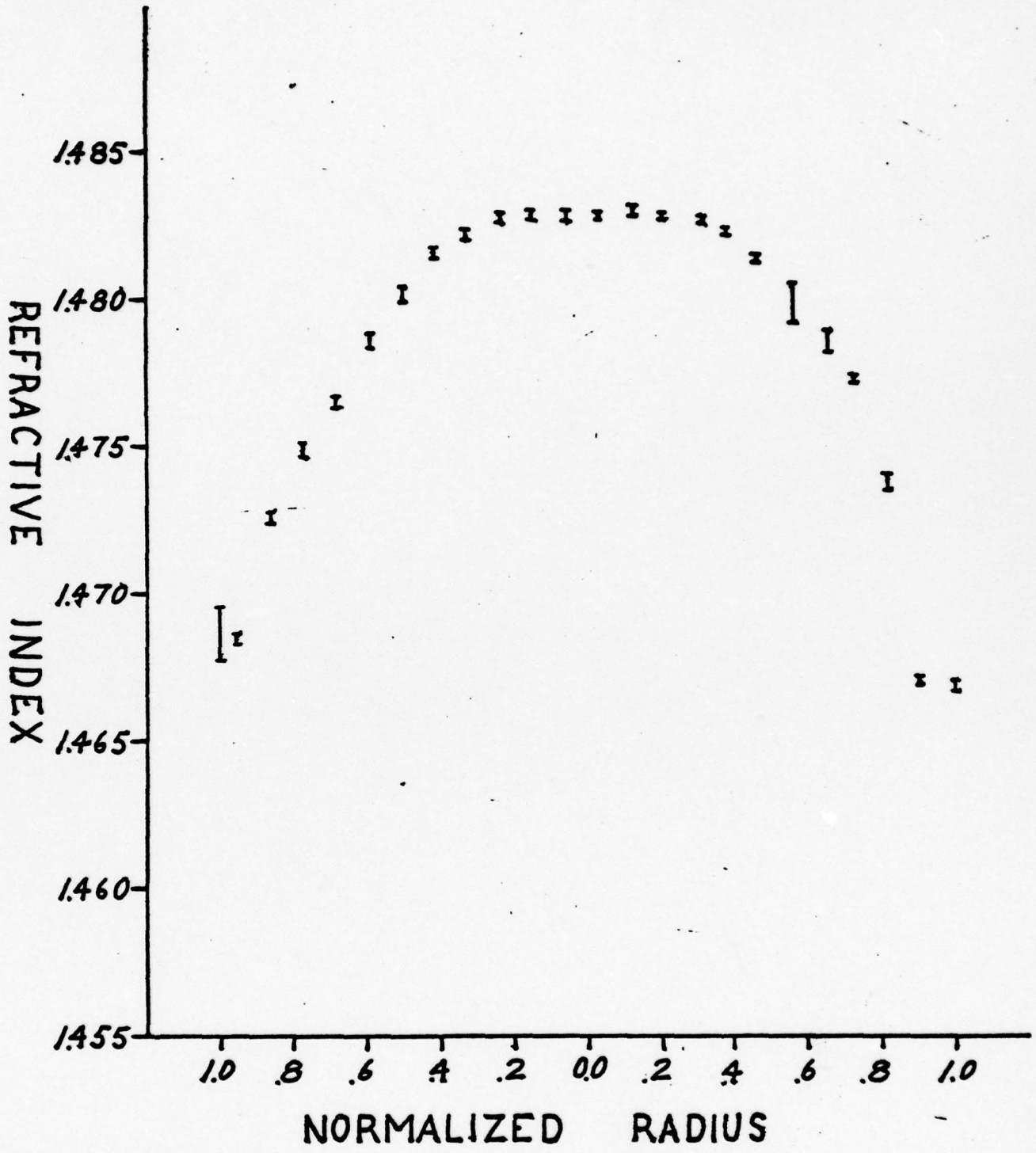

Fig. 12. The profile of a preform prepared from a homogeneous glass rod. The profile has a flat top and high edges.

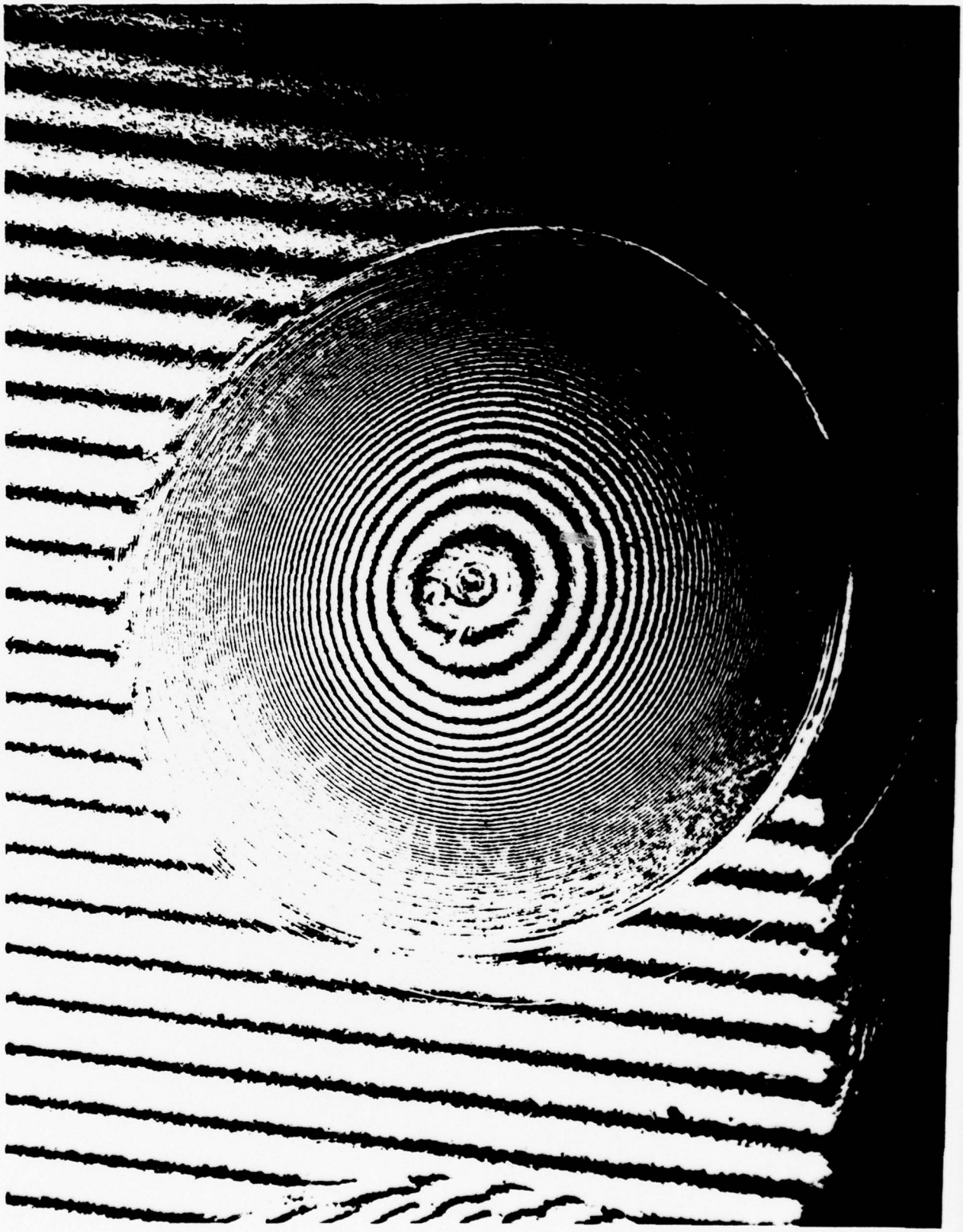

Fig. 13. Interferogram of a rod having a poor profile but showing good homogeneity in the base glass.

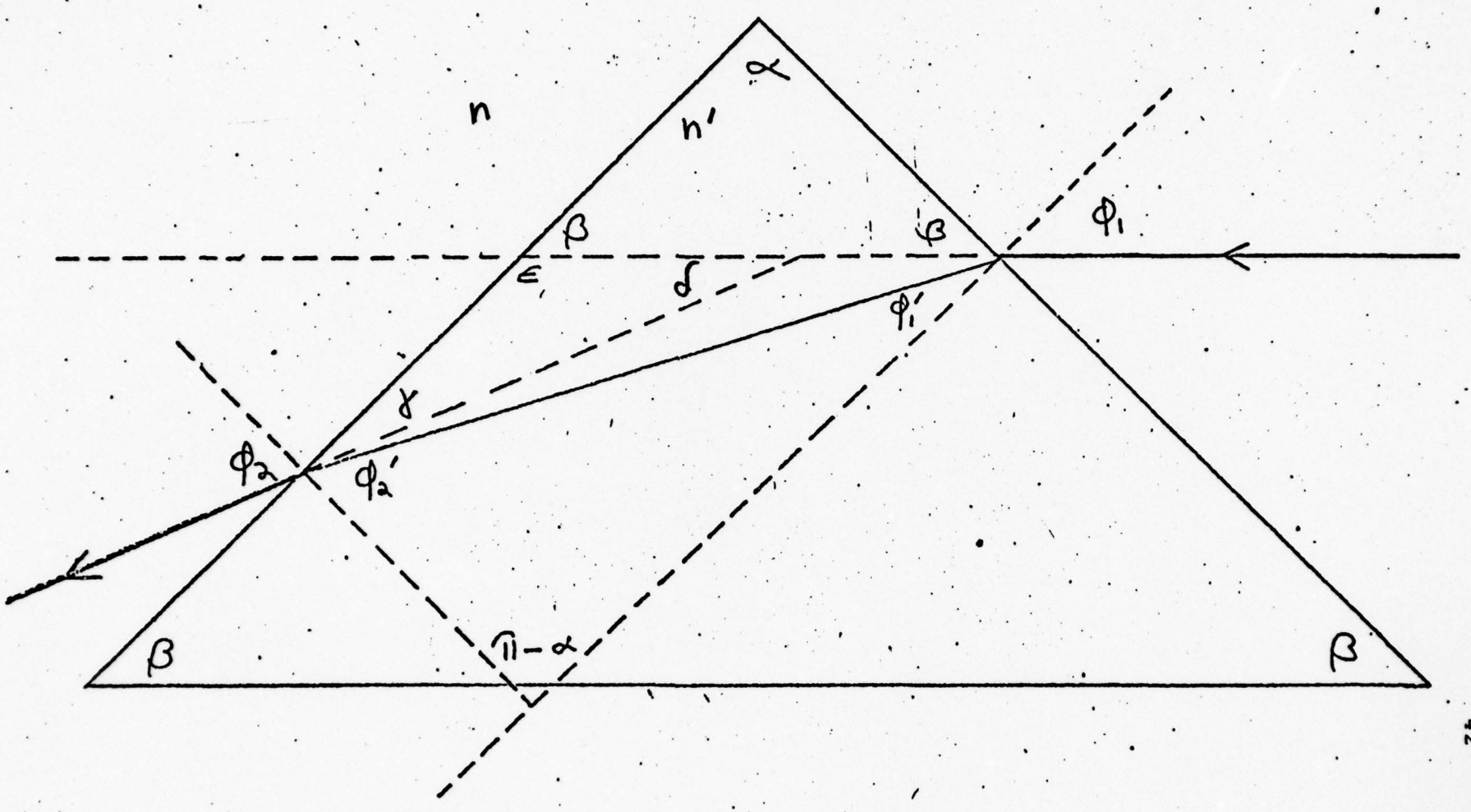

Fig. 14. PRISM GEOMETRY FOR INDEX MEASUREMENT

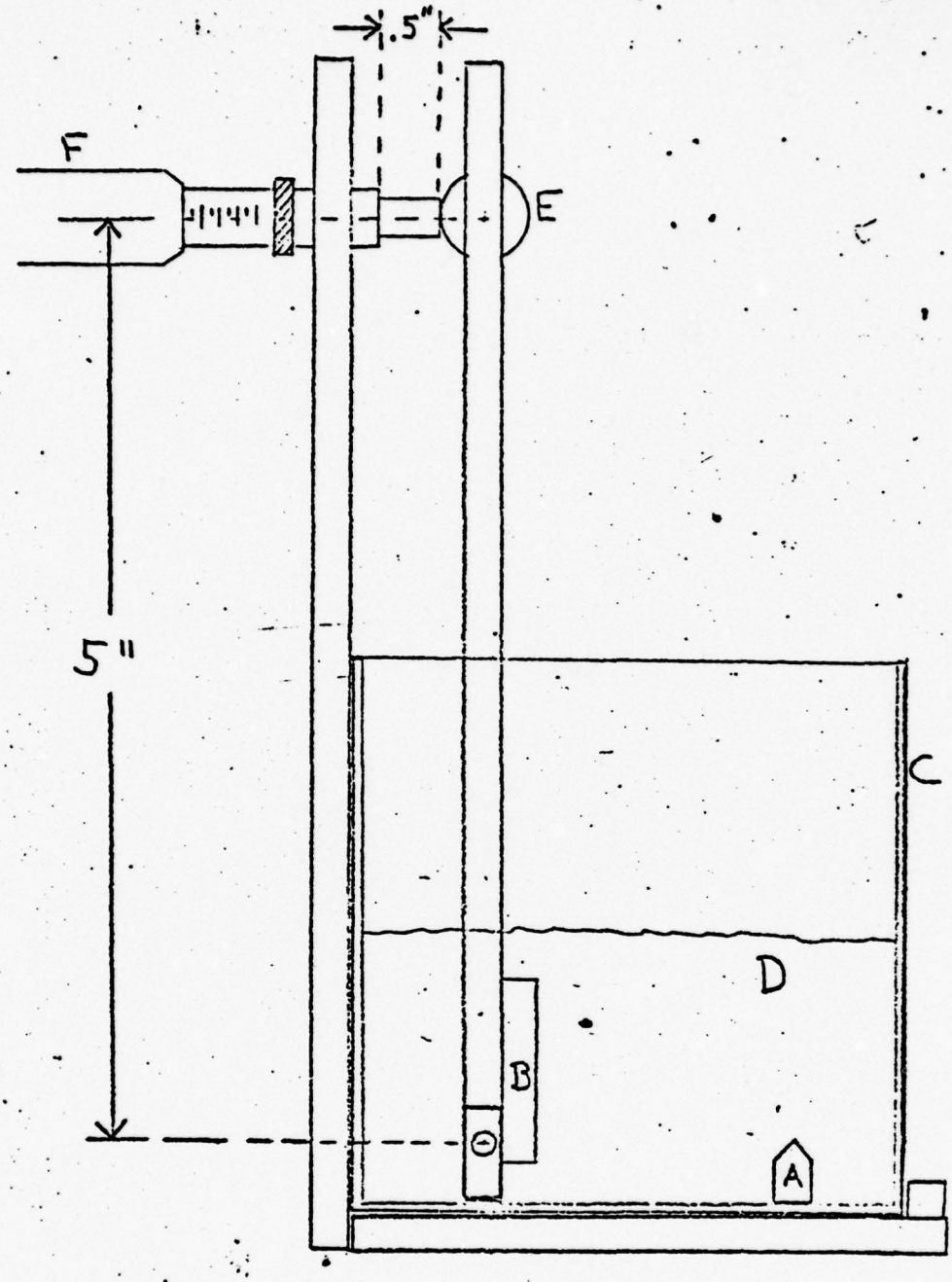

Fig. 15. Index Profile Measuring Apparatus

Figure 15: Index Profile Measuring Apparatus

A. Sample Prism

B. Mirror

C. Optical Cell

D. Matching Fluid - Paraffin Oil

E. Ball bearing, $\approx$ 1/2 diameter

F. Micrometer

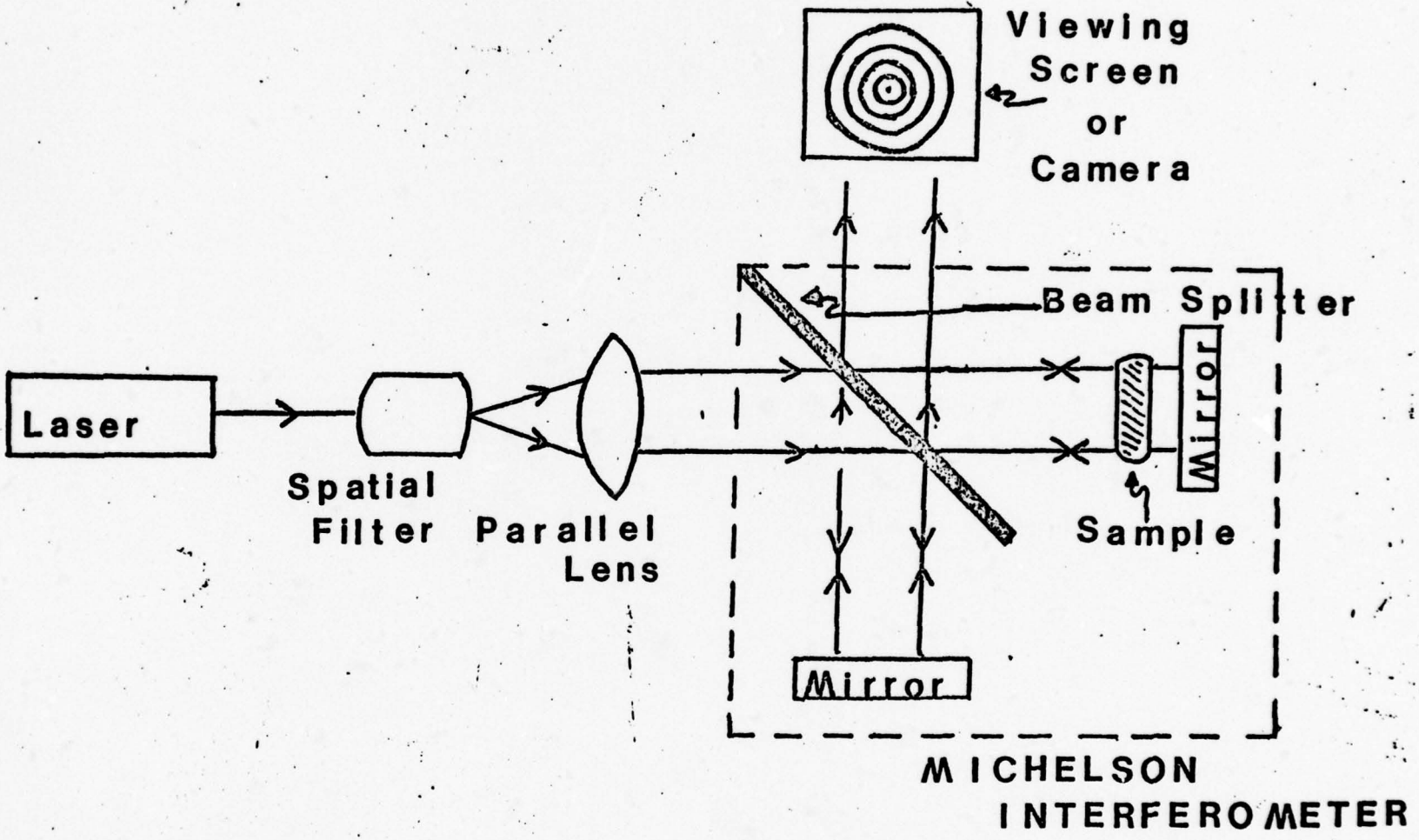

Figure 16. Michelson Interferometer

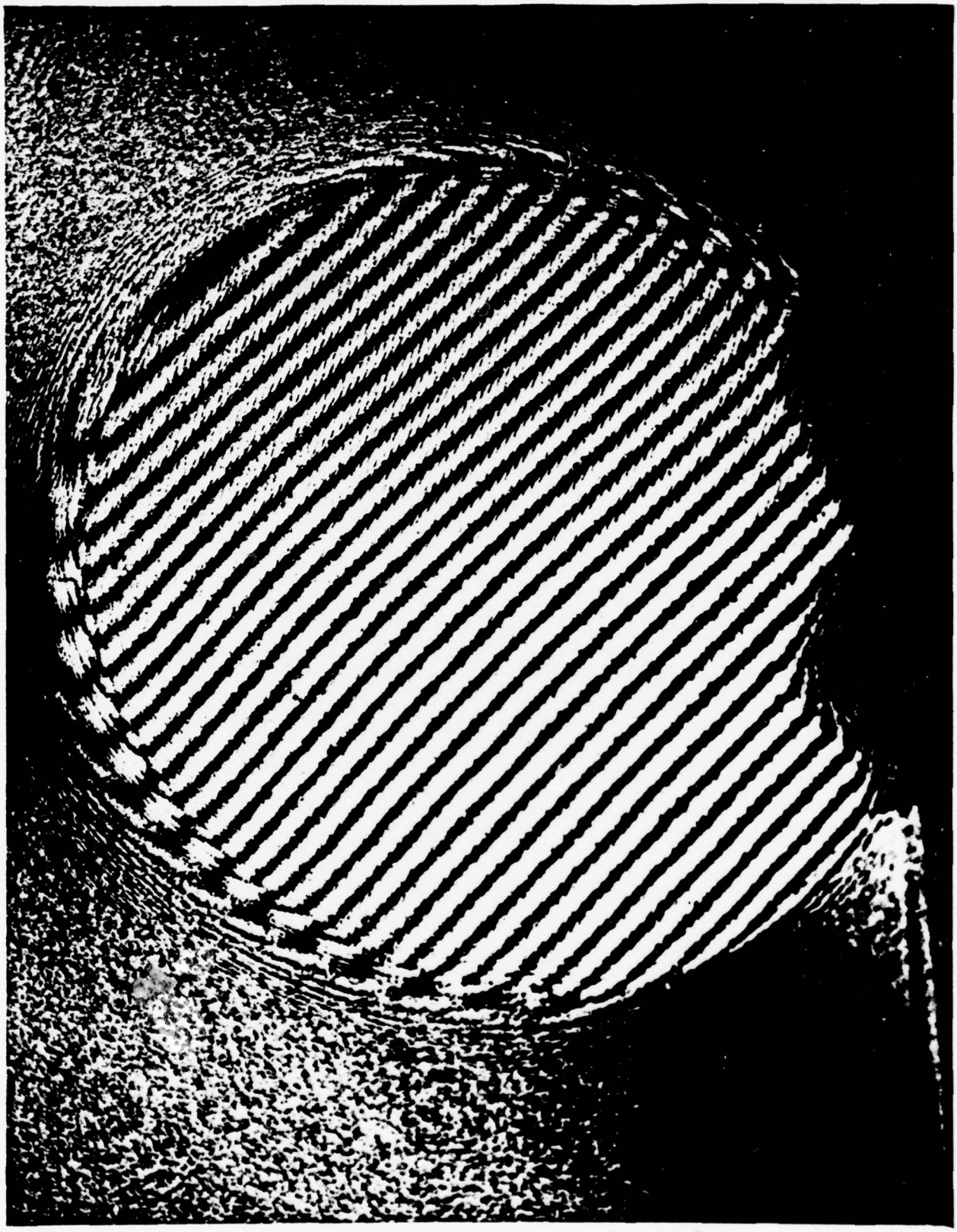

Figure 17. Interferogram of the homogeneous base glass.

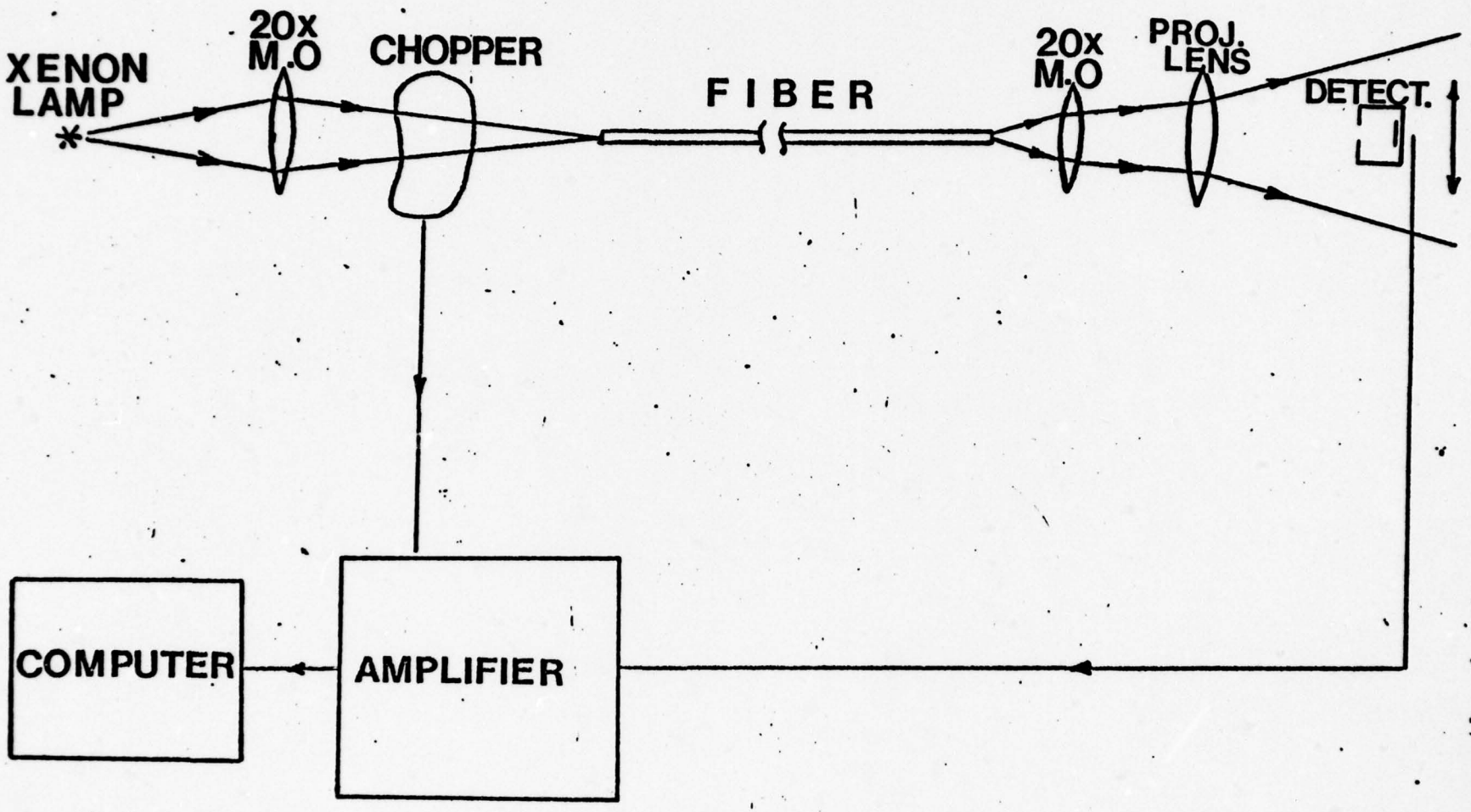

Figure 18. Schematic of the near field index measuring apparatus.

Figure 19.

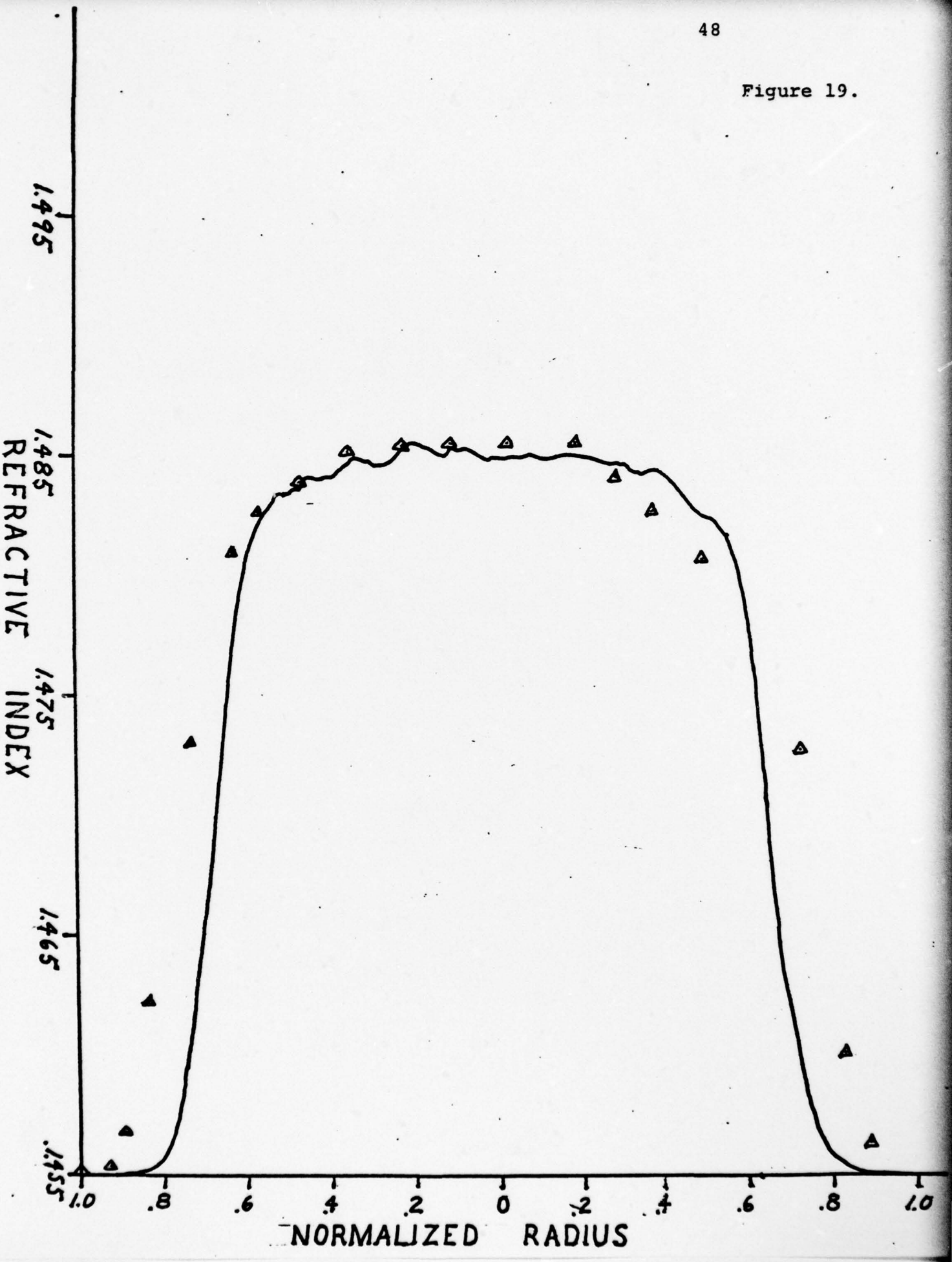
1.495
1.485
1.475
1.465
1.455
REFRACTIVE INDEX
1.0
.8
.6
.4
.2
0
.2
.4
.6
.8
1.0
NORMALIZED RADIUS

Figure 19.

The solid line is the plot of the index profile of a fiber measured using the near field technique. The triangular data points show the profile of the rod from which the fiber was drawn.

Fig. 20

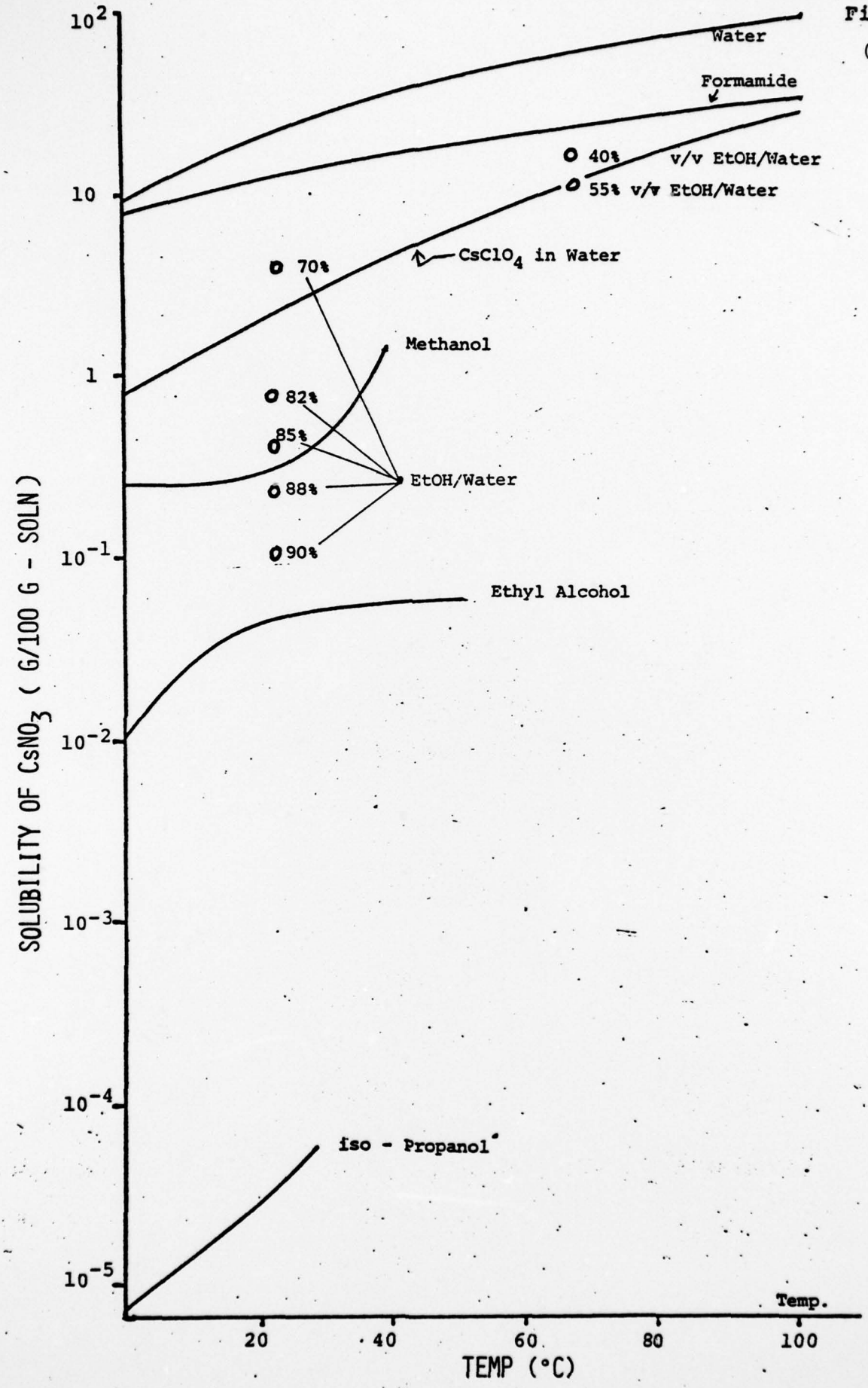
Water
Formamide
40% v/v EtOH/Water
55% v/v EtOH/Water
$CsClO_4$ in Water
70%
Methanol
82%
85%
EtOH/Water
88%
90%
Ethyl Alcohol
iso - Propanol
10^2
10
1
10^{-1}
10^{-2}
10^{-3}
10^{-4}
10^{-5}
SOLUBILITY OF $CsNO_3$ (G/100 G - SOLN)
Temp.
20
40
60
80
100
TEMP (°C)

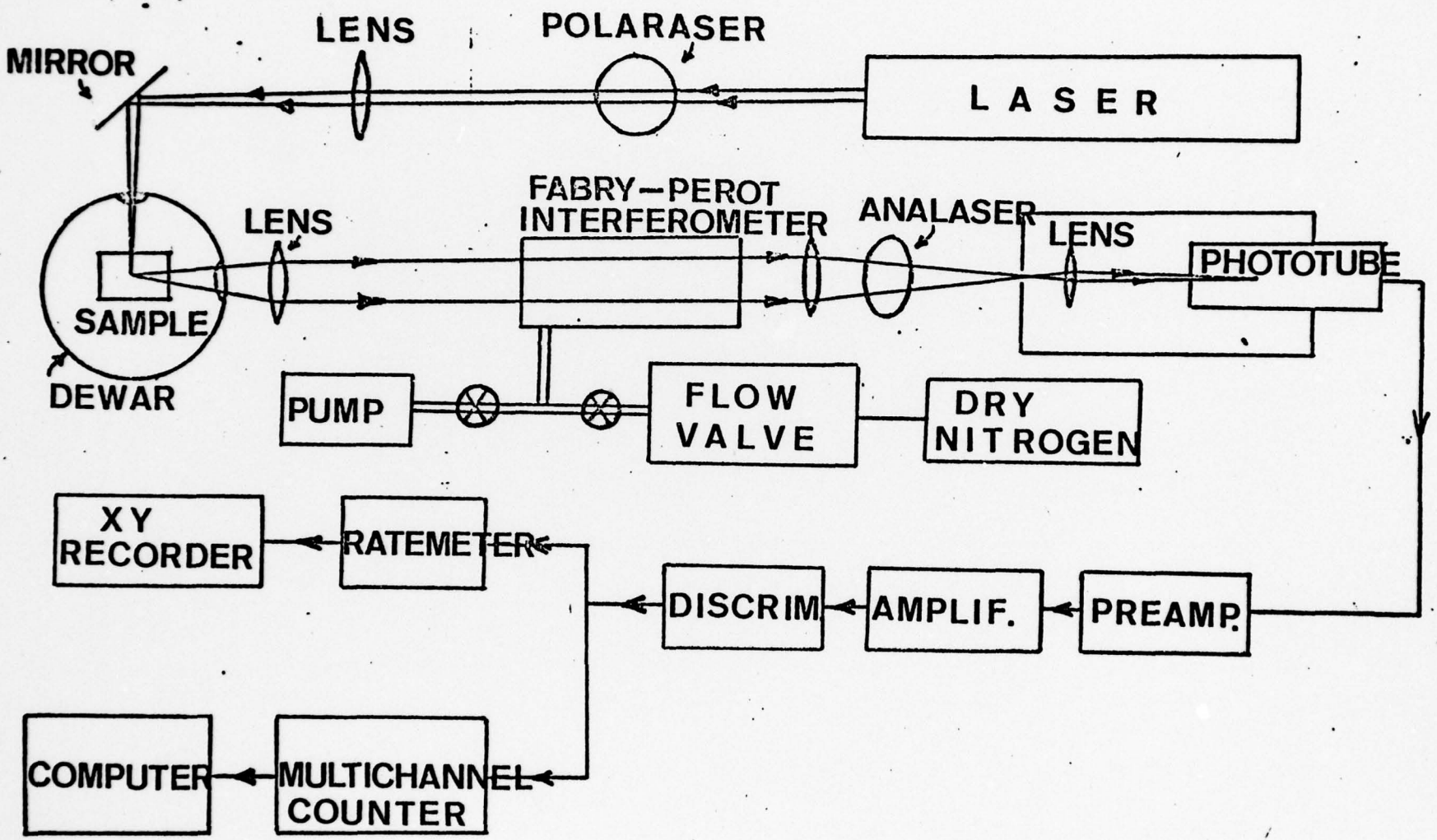

Figure 21. Schematic of the Landau-Placzek Measuring Apparatus.

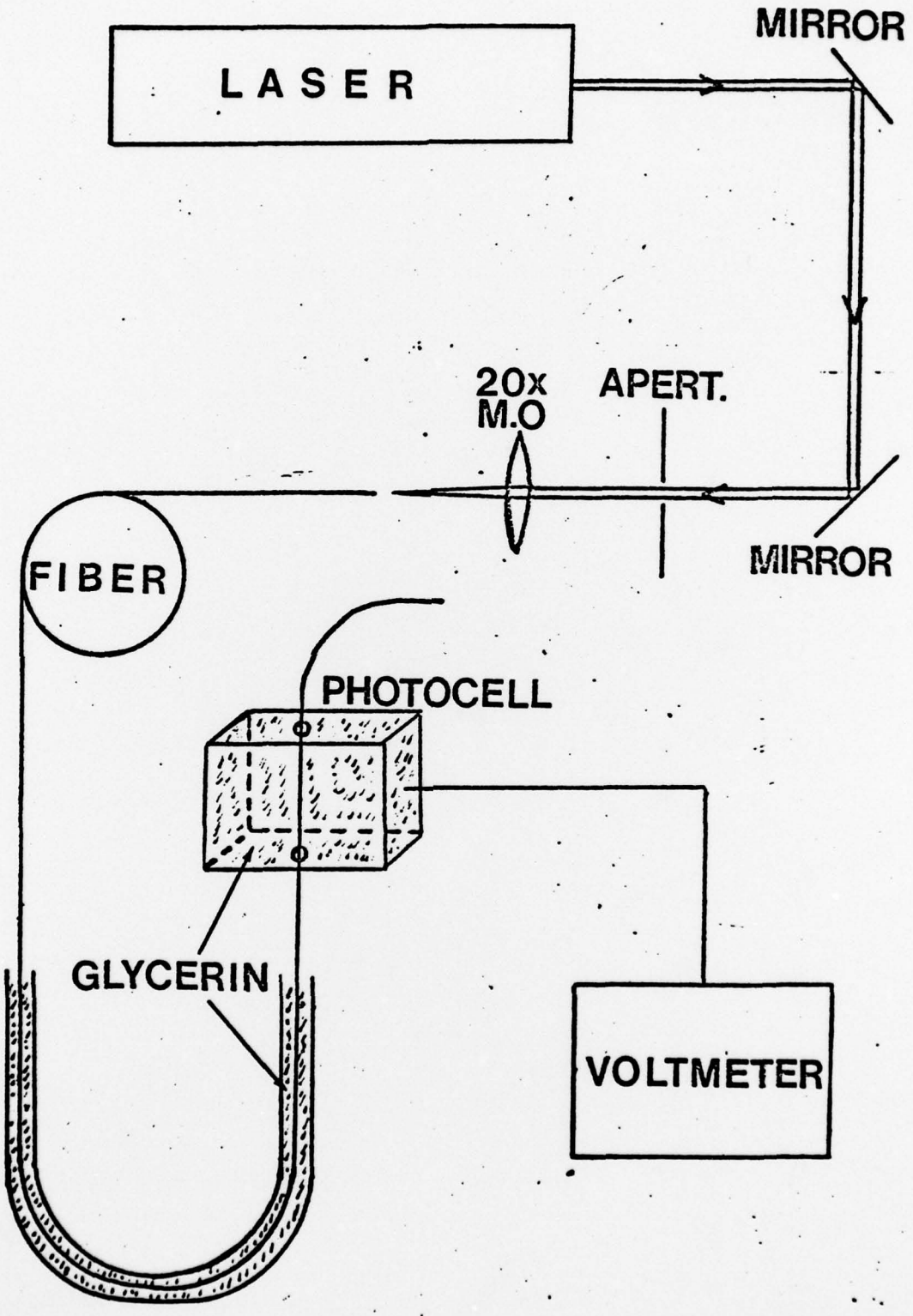

Figure 22. Schematic of the total scattering measuring apparatus.

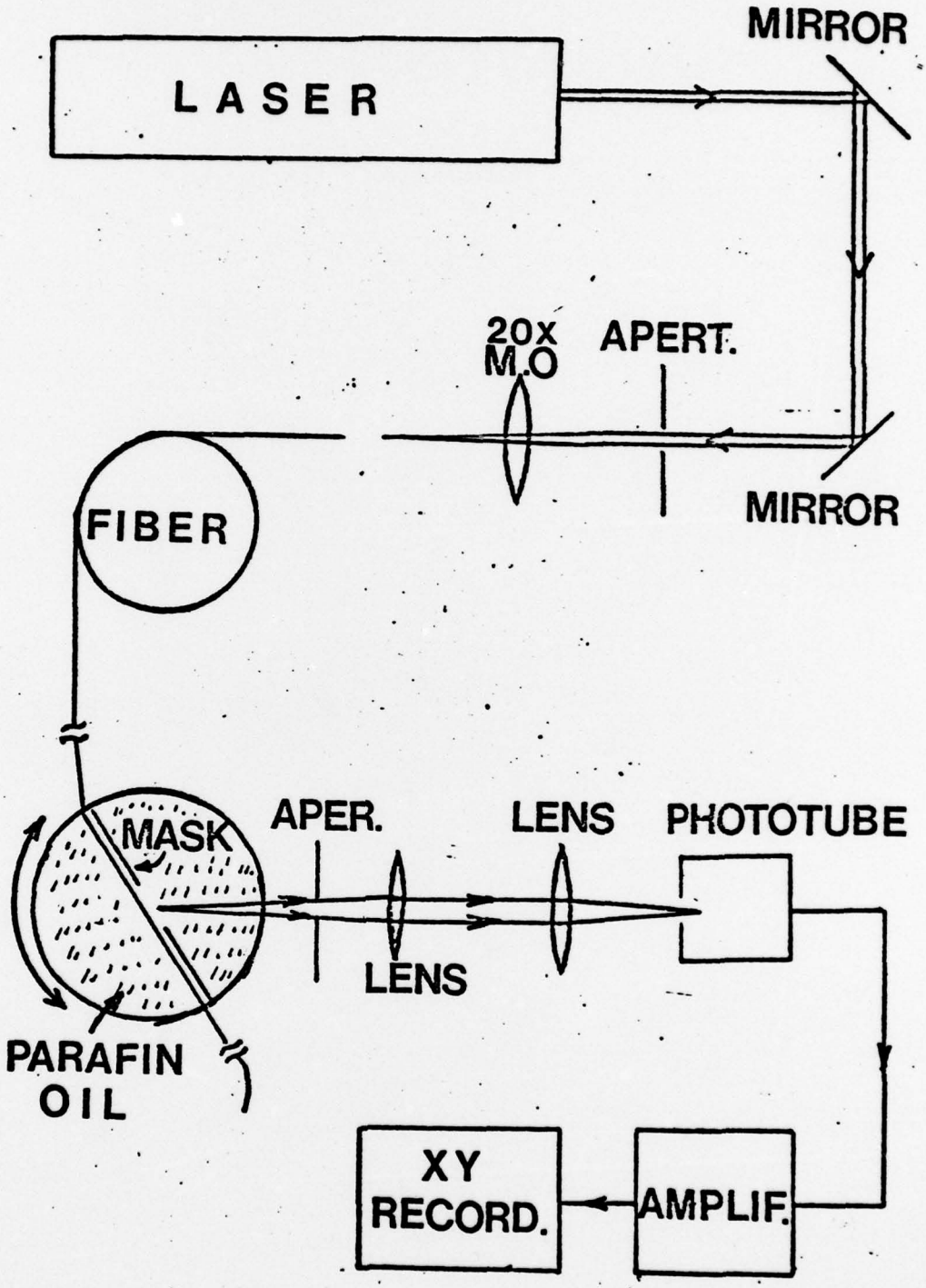

Figure 23. Schematic of the apparatus for measuring the angular distribution of scattered light.

Fig. 24

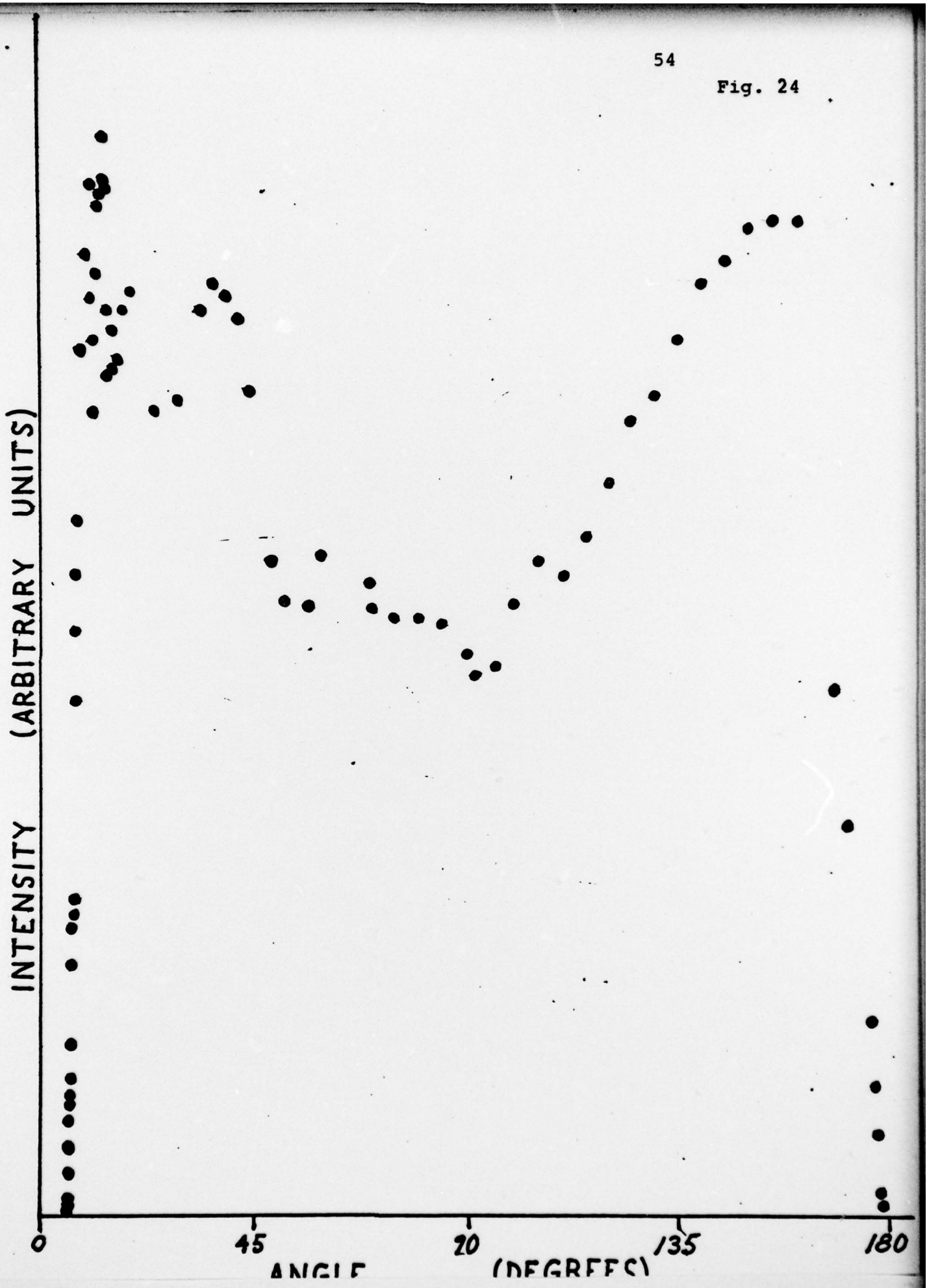

Figure 24. The angular distribution of light scattered from a fiber section exhibiting only the $1 + \cos^2\theta$ dependence due to Rayleigh Scattering. The $1 + \cos^2\theta$ shape is distorted due to refraction at the core clad and clad oil interfaces. The noisy signal in the near forward direction is due to the difficulty of collecting the light scattered in the forward direction.

Fig. 25

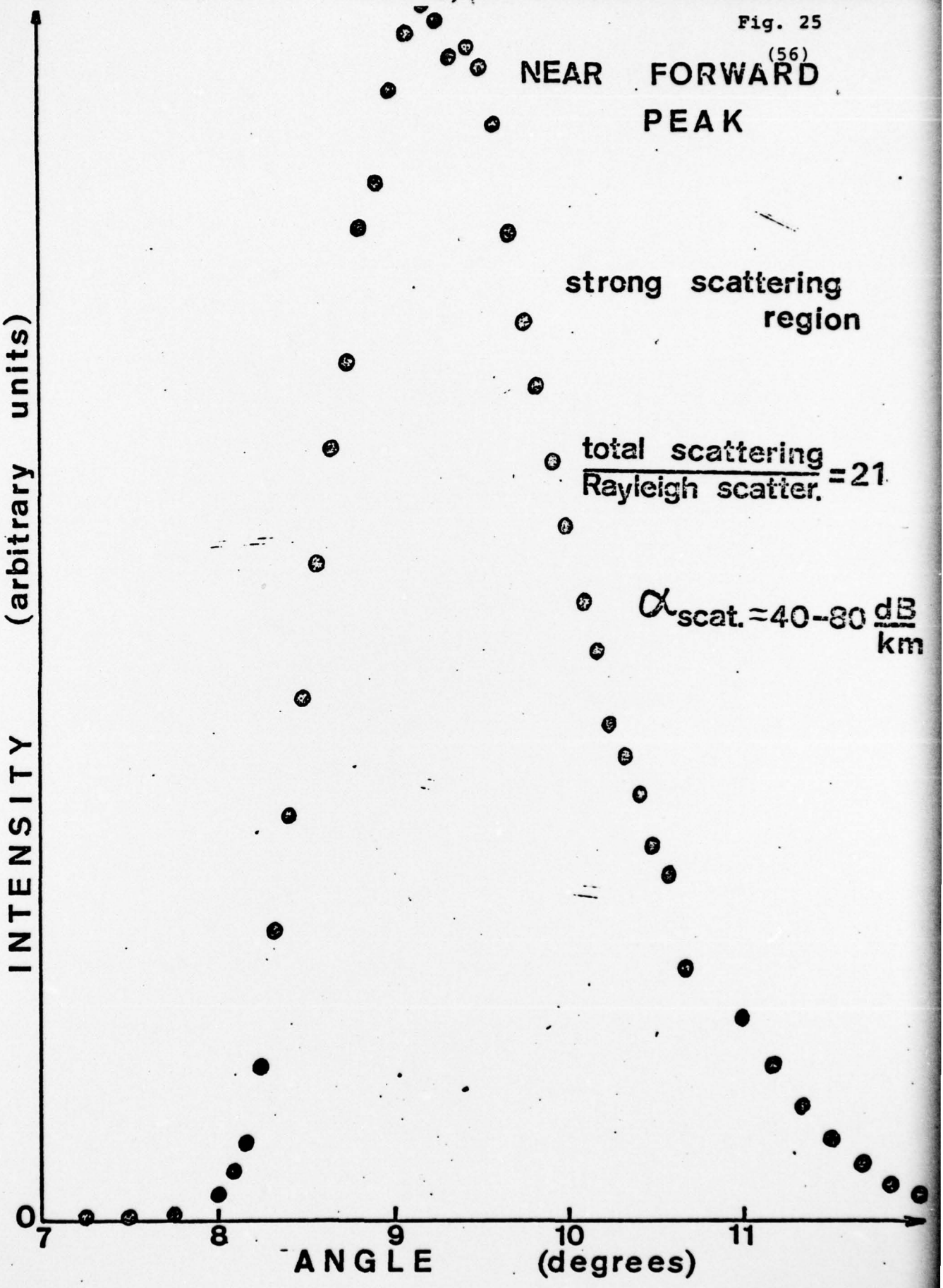
NEAR FORWARD PEAK
strong scattering region
total scattering / Rayleigh scatter. = 21
$\alpha_{scat.} \approx 40\text{-}80 \frac{dB}{km}$
INTENSITY (arbitrary units)
0
7
8
9
10
11
ANGLE (degrees)

Figure 25. The forward scattering peak of a strong scattering region of a fiber. The intensity scattered into the forward peak is 21 times that due to the integrated Rayleigh scattering alone.

Figure 26.

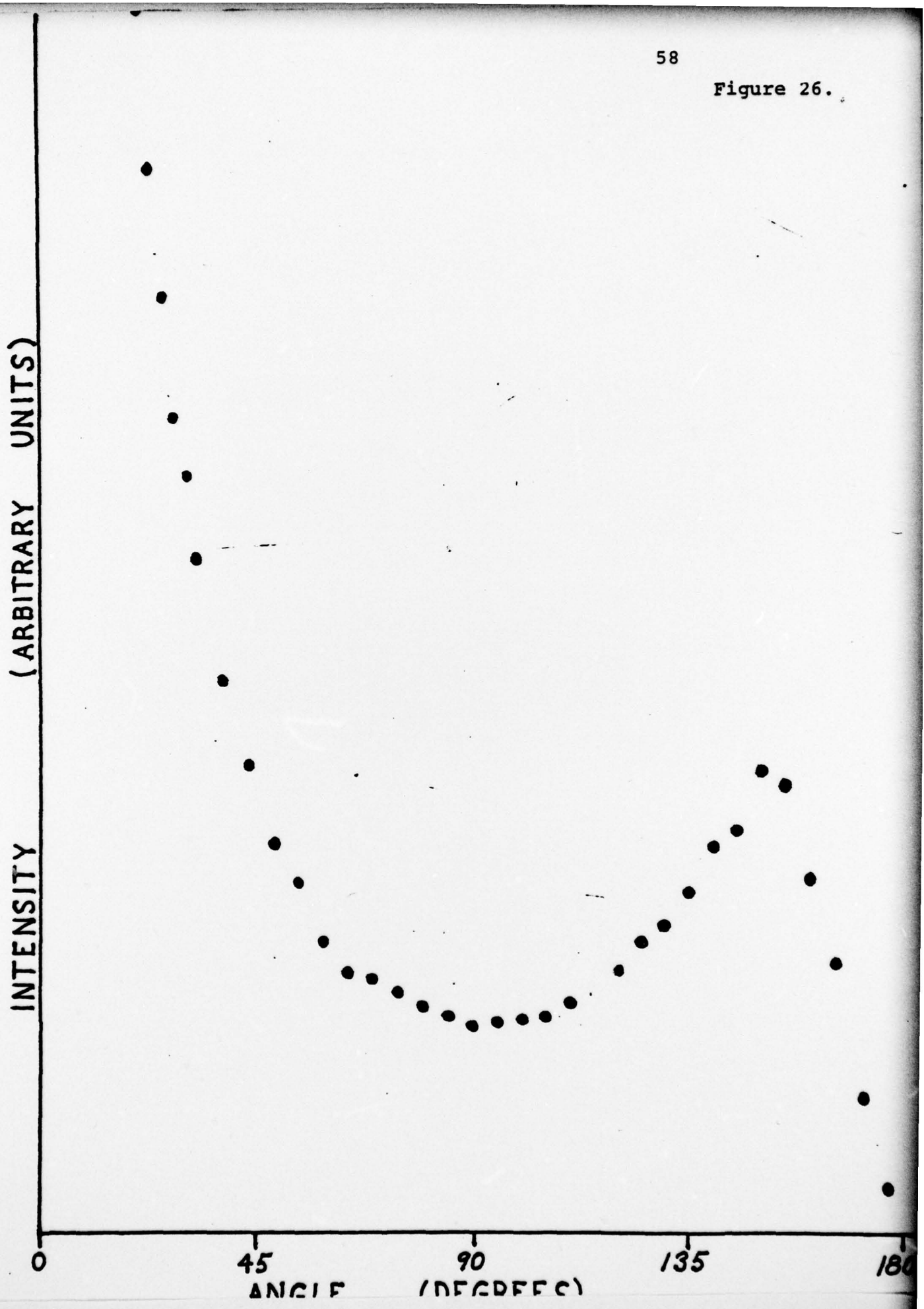

Figure 26. The angular distribution of light scattered from a strong scattering region in a fiber. The forward peak is offscale in this plot.

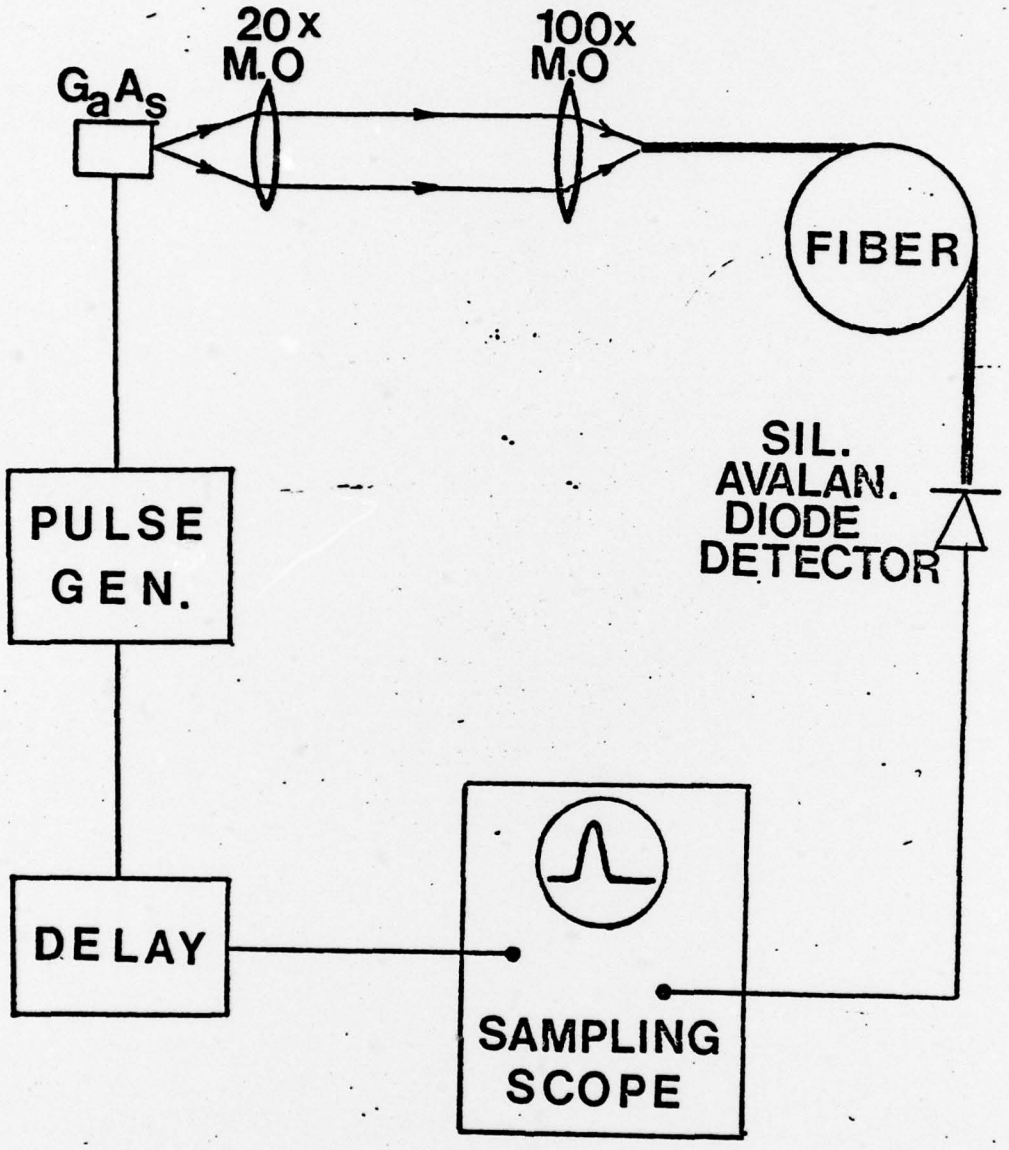

Figure 27. Schematic of the Dispersion Measuring Apparatus

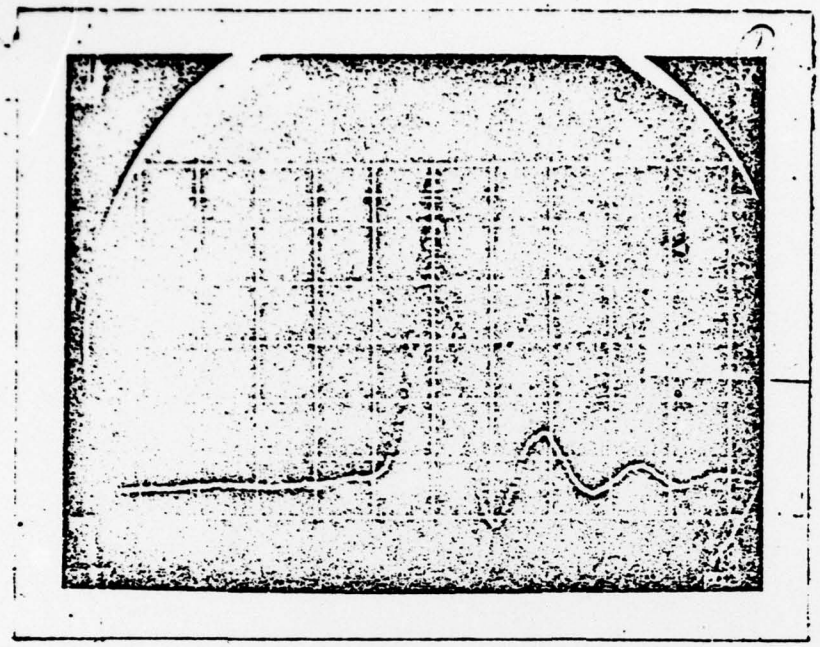

a.

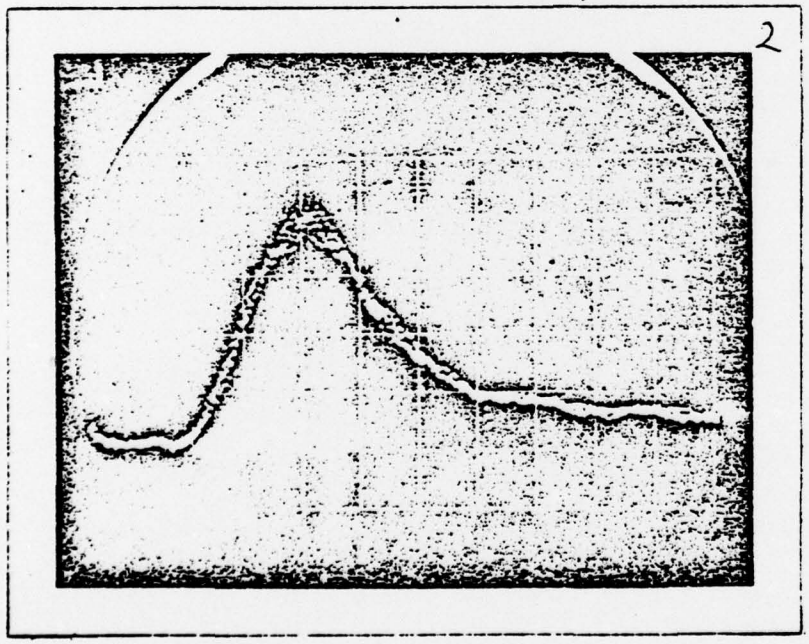

b.

Figure 28a shows the unbroadened instrumental peak.

28b shows the broadening observed after transmission through 1 km of fiber.

REFERENCES

1. B. Costa, B. Sordo, Second European Conference on Optical Fiber Communication, Paris, 1976

2. J. Schroeder, R. Mohr, P.B. Macedo and C.J. Montrose, J. Amer. Ceram. Soc. 56, 510 (1973)

3. T.C. Rich and D.A. Pinnow, Appl. Phys. Lett. 20 264 (1972)

4. A.R. Tynes, Appl. Opt. 9 2706 (1970)

5. E.G. Rawson, Appl. Opt. 11 2477 (1972)

6. J.R. Andrews, Rev. Sci. Instrum. 45 22 (1974)